







RESEARCH ARTICLE

Capacity of deep-sea corals to obtain nutrition from cold seeps aligned with microbiome reorganization

Eslam O. Osman^{1,2,3}  | Samuel A. Vohsen¹  | Fanny Girard^{1,4}  | Rafaelina Cruz¹ | Orli Glickman¹ | Lena M. Bullock¹ | Kaitlin E. Anderson¹ | Alexis M. Weinnig⁵  | Erik E. Cordes⁵  | Charles R. Fisher¹ | Iliana B. Baums^{1,6} 

¹Department of Biology, The Pennsylvania State University, State College, Pennsylvania, USA

²Marine Biology Lab, Zoology Department, Faculty of Science, Al-Azhar University, Cairo, Egypt

³Red Sea Research Center (RSRC), King Abdullah University of Science and Technology (KAUST), Thuwal, Saudi Arabia

⁴Monterey Bay Aquarium Research Institute, Moss Landing, CA, USA

⁵Biology Department, Temple University, Philadelphia, PA, USA

⁶Helmholtz Institute for Functional Marine Biodiversity (HIFMB), Ammerländer, Heerstraße 231, 26129 Oldenburg, Germany

Correspondence

Eslam O. Osman and Iliana B. Baums, Department of Biology, The Pennsylvania State University, State College, PA, USA. Email: eom.osman@gmail.com and iliana.baums@hifmb.de

Funding information

Ecosystem Impacts of Oil and Gas Inputs to the Gulf (ECOGIG), Grant/Award Number: 572

Abstract

Cold seeps in the deep sea harbor various animals that have adapted to utilize seepage chemicals with the aid of chemosynthetic microbes that serve as primary producers. Corals are among the animals that live near seep habitats and yet, there is a lack of evidence that corals gain benefits and/or incur costs from cold seeps. Here, we focused on *Callogorgia delta* and *Paramuricea* sp. type B3 that live near and far from visual signs of currently active seepage at five sites in the deep Gulf of Mexico. We tested whether these corals rely on chemosynthetically-derived food in seep habitats and how the proximity to cold seeps may influence; (i) coral colony traits (i.e., health status, growth rate, regrowth after sampling, and branch loss) and associated epifauna, (ii) associated microbiome, and (iii) host transcriptomes. Stable isotope data showed that many coral colonies utilized chemosynthetically derived food, but the feeding strategy differed by coral species. The microbiome composition of *C. delta*, unlike *Paramuricea* sp., varied significantly between seep and non-seep colonies and both coral species were associated with various sulfur-oxidizing bacteria (SUP05). Interestingly, the relative abundances of SUP05 varied among seep and non-seep colonies and were strongly correlated with carbon and nitrogen stable isotope values. In contrast, the proximity to cold seeps did not have a measurable effect on gene expression, colony traits, or associated epifauna in coral species. Our work provides the first evidence that some corals may gain benefits from living near cold seeps with apparently limited costs to the colonies. Cold seeps provide not only hard substrate but also food to cold-water corals. Furthermore, restructuring of the microbiome communities (particularly SUP05) is likely the key adaptive process to aid corals in utilizing seepage-derived carbon. This highlights that those deep-sea corals may upregulate particular microbial symbiont communities to cope with environmental gradients.

KEYWORDS

16S metabarcoding, deep sea, microbiome, stable isotopes, SUP05, transcriptomes

This is an open access article under the terms of the [Creative Commons Attribution-NonCommercial-NoDerivs](https://creativecommons.org/licenses/by-nc-nd/4.0/) License, which permits use and distribution in any medium, provided the original work is properly cited, the use is non-commercial and no modifications or adaptations are made.

© 2022 The Authors. *Global Change Biology* published by John Wiley & Sons Ltd.

1 | INTRODUCTION

Cold-water coral communities are diverse and abundant in the deep sea. Corals increase habitat heterogeneity and provide a three-dimensional framework for many invertebrate and fish species (Cho & Shank, 2010; Cordes et al., 2008). Cold-water corals are long-lived and slow growing species, and thus, they are vulnerable to natural and anthropogenic threats (Clark et al., 2016; Thresher et al., 2015; Weinnig et al., 2020). For example, hydrocarbon pollution has long-term impacts on coral health and the associated fauna (Girard et al., 2018; Guzman et al., 2020; McClain et al., 2019). Exposure to hydrocarbons and related toxic chemicals may cause colony mortality or have sublethal consequences such as; (i) a decline in health and growth of coral colonies (Girard & Fisher, 2018; Girard et al., 2019), (ii) a change of the associated epifauna (Demopoulos et al., 2016; Lewis et al., 2020), (iii) a shift in the associated microbial community (Luter et al., 2019; Turner & Renegar, 2017), and (iv) an influence on gene expression of the coral host (DeLeo et al., 2018, 2021). Yet, some cold-water corals grow near active cold seeps (Quattrini et al., 2013) that are a source of various chemicals including hydrogen sulfide, methane, and other hydrocarbon-rich fluids in the environment. The presence of these chemicals raises the question of whether coral species utilize seepage effluents and/or acclimatize to seepage exposure in some way.

At cold seeps, hydrocarbons naturally leak from the sea floor over a few to hundreds of square meters. Microbial processing of the leaked hydrocarbons results in authigenic carbonates that serve as reef-like habitats and are settled by many invertebrates (see Joye, 2020). Chemosynthetic microbes also use seeping chemicals to produce organic carbon and so act as primary producers for cold seep communities (Joye, 2020). Generally, cold seep community members benefit from the higher food availability near seeps relative to background habitats, but detoxification of seep effluent may be necessary and energetically costly. Some animals use metabolic detoxification pathways in their tissue to convert hydrocarbons to simpler compounds (e.g., alcohols and ketones—see Kennicutt, 2017). Other animals associate with chemosynthetic microbes (Fisher et al., 2007) that convert toxic to non-toxic substances and fix carbon (Laso-Pérez et al., 2019; Niemann et al., 2013; Sogin et al., 2020). Most cold seep fauna (e.g., siboglinid tubeworm, bathymodiolus mussels) have chemosymbiotic microbes and/or upregulate expression of genes related to the innate immune system, heavy metal detoxification, and metabolic pathways involving sulfide when toxic chemicals are present in the environment (Cheng et al., 2019; Osman & Weinnig, 2022; Sogin et al., 2020; Wong et al., 2015).

A number of coral species live near cold seeps (e.g., *Lophelia pertusa*, *Balanophyllia* sp.) in different biogeographic regions, but it is not clear what benefits corals gain from living near cold seep habitats (Deng et al., 2019; Hovland & Thomsen, 1997). In a single laboratory study, the holobiont of the deep-sea scleractinian coral *L. pertusa* was shown to be capable of chemoautotrophy and nitrogen fixation (Middelburg et al., 2015), but the microbes responsible

for these processes and the degree to which they supply nutrition in situ remains unresolved. So far, the influence of cold seeps on these corals appears limited. In fact, most deep-sea organisms rely on photosynthetic detritus sunk from photic/shallow water or other organisms that feed on surface-derived food (McClain-Counts et al., 2017). Previous stable isotope studies showed that photosynthetic-derived food is the major food source in deep-sea corals, even near cold seeps (e.g., Becker et al., 2009). A signature of chemosynthetically derived food in their tissue or a mechanism to adapt to cold seeps has not been found (Rincón-Tomás et al., 2019; Xu et al., 2019). Therefore, it was proposed that coral species mainly occupy seep habitats because the authigenic carbonates provide suitable substrate but only after the seepage has largely faded and hydrocarbons/oil are no longer released. Nevertheless, the octocorals *Callogorgia delta* (200–1000m) and *Paramuricea* spp. (835–1090m) occasionally grow in very close proximity (within a few meters) to areas of active seepage in the Gulf of Mexico (Doughty et al., 2014; Quattrini et al., 2013). Indeed, *C. delta* and *Paramuricea* sp. type B3 have been observed living amid bacterial mats and near dead mussel beds that relied on active seepage (Figure 1). This observation suggests that certain coral populations may be exposed to active seepage and be able to utilize and/or tolerate cold seeps like other seep fauna.

Here, we focus on these coral populations and use proximity to signs of active seepage as an indicator of exposure to seep effluents. We assessed to what extent these corals gain benefits from living near cold seeps and whether they rely on food with a chemosynthetic and/or photosynthetic origin. We compared colony and holobiont traits as an indicator of metabolic benefits or cost imposed by exposure to seepage. *C. delta* and *Paramuricea* sp. type B3 were imaged and collected from five sites in the Gulf of Mexico near and far from signs of active seepage. Bulk carbon and nitrogen stable isotope composition of tissue was analyzed to differentiate between chemo- and photosynthetic origin. We assessed coral health status, growth rates, branch loss, and how well coral colonies recovered from sampling (cutting injury) as a proxy for energetic reserves. Also, we characterized the associated epifauna and microbiome composition and analyzed host gene expression relative to signs of active seepage. We report that these corals obtain some of their nutrition from a chemosynthetically derived food source whose origin appears to vary between coral species. While the composition of the microbial communities of *C. delta* and sediment samples changed significantly between seep and non-seep sites, we could not detect a measurable impact of cold seeps on coral fitness traits, associated epifauna, or the host transcriptome. Our study provides the first evidence that corals living near cold seeps not only use seep habitats for substrate, but also feed on chemosynthetic food similar to other seep fauna, without experiencing negative impacts on the measured coral colony traits or on the composition of associated epifauna communities. A shift in microbial community composition, particularly the SUP05 group, is likely a key adaptive mechanism that enabled those coral colonies to utilize and/or tolerate cold seeps.

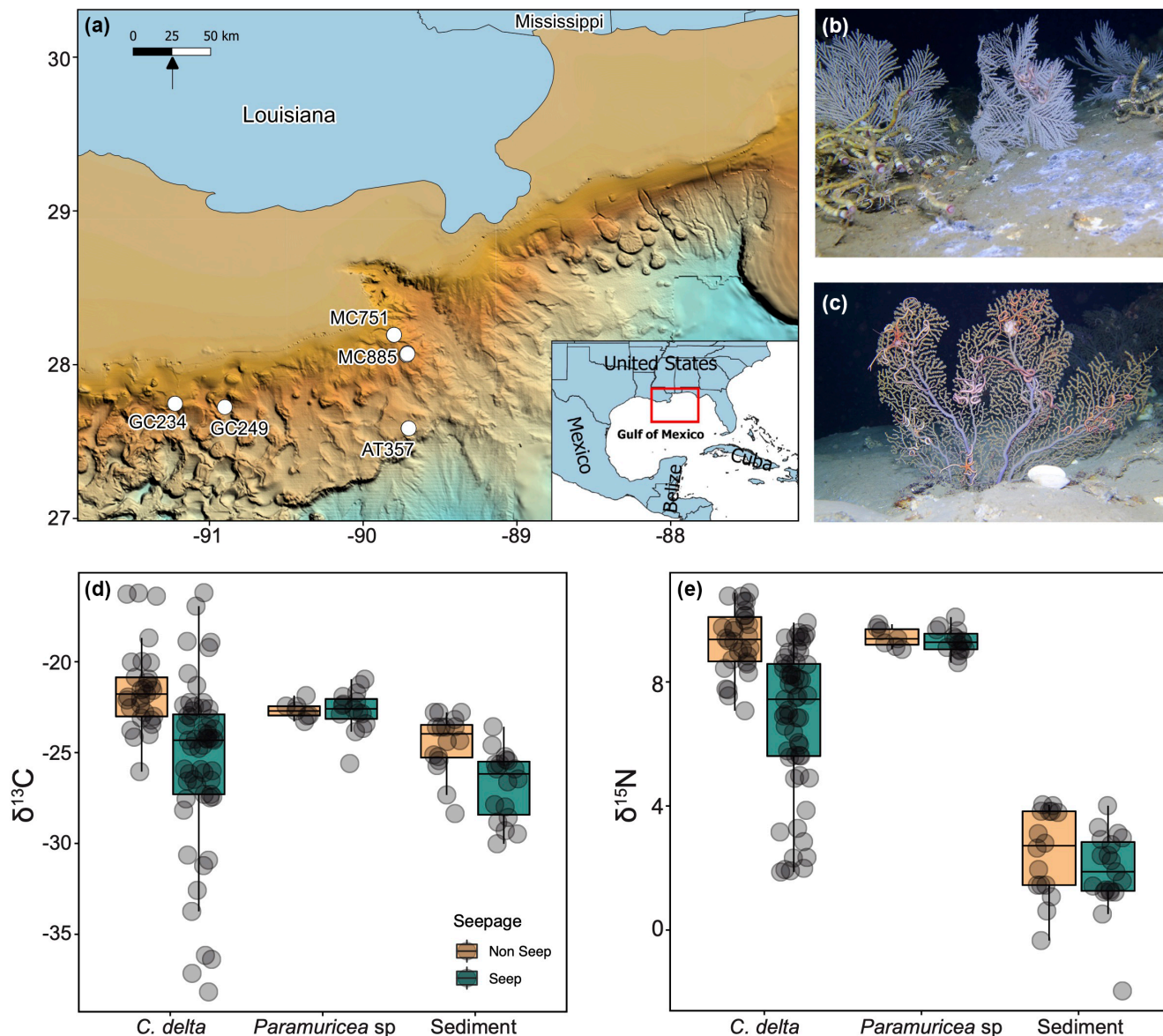


FIGURE 1 Map shows sampling sites of *Collogorgia delta* and *Paramuricea* sp. collected from cold seep and non-seep from five sites in the Gulf of Mexico (a). Colonies of *C. delta* (b) and *Paramuricea* sp. (c) were found near active and far from active cold seep. Coral colonies were sampled and photographed to assess the impact of cold seeps on corals health, growth rate, regrowth after sampling, branch loss, and associated epifauna. Colonies were also sampled to assess the microbiome community and host gene expression. Boxplots and point clouds represent the range of carbon $\delta^{13}\text{C}$ (d) and nitrogen $\delta^{15}\text{N}$ (e) stable isotope values (‰) in *C. delta*, *Paramuricea* sp. and sediment in cold seep (teal) and non-seep (orange) samples collected from five sites in the Gulf of Mexico. Stable isotope values demonstrate significant differences between seep and non-seep samples in *C. delta* and sediment samples ($\delta^{13}\text{C}$ value < -23 indicates chemosynthesis), but not in *Paramuricea* sp., highlighting chemosynthetic signatures.

2 | MATERIALS AND METHODS

2.1 | Study sites

Five sites ranging from 450 to 1050m depth were surveyed in the Gulf of Mexico. Sites were MC751, MC885, GC234, GC249, and AT357, named corresponding to Bureau of Ocean Energy Management (BOEM) designations of the Lease Blocks in which the sites are located (Figure 1, MC—Mississippi Canyon, GC—Green Canyon, AT—Atwater Valley). Surveys were conducted

using remotely operated vehicles (ROV) onboard the vessels E/V Nautilus (April–June 2015, ROV Hercules), DSV Ocean Inspector (September–October 2016, ROV Global Explorer), and MSV Ocean Intervention II (April–June 2017, ROV Global Explorer). ROVs were deployed to survey cold seeps at each site (Table S1). Cold seeps were visually identified from ROV livestream high resolution video footage using one of the following visual indicators; (i) gas bubbles indicating active/eruptive seepage (rarely observed), (ii) patchy white and/or orange bacterial mats of the genera *Sulfurimonas*, *Sulfurovum*, and/or *Beggiatoa* indicating localized diffusion of

hydrogen sulfide and/or methane (Joye et al., 2004), (iii) the presence of cold seep foundation species indicating access to methane/hydrogen sulfide (Bathymodiolin mussels, Vesicomid clams or Siboglinid tubeworms—Fisher et al., 2007). Coordinates were taken for each of the seep and non-seep (no visible signs of seepage) locations and a marker deployed for unambiguous relocation in future years. At each seep and non-seep marker, we collected the following data: (i) photographs of *C. delta* and *Paramuricea* sp. type B3 colonies to assess the impact of cold seeps on visual health status, growth rates, and the composition of associated epifauna. (ii) coral tissue, surrounding seawater, and sediment samples to assess holobiont composition (microbiome and host transcriptomes) as well as to quantify the stable isotopic composition of carbon and nitrogen in coral tissue and sediments. (iii) measurement of seawater temperature, salinity, oxygen concentration, and depth (except 2016 due to logistical difficulties) at each sampling point using calibrated sensors mounted on the ROV. All statistics were conducted using “R” statistical software with default parameters unless otherwise stated (R Development Core Team, 2017).

2.2 | Study species and visual fitness traits

We focused on two soft coral species, *C. delta* and *Paramuricea* sp. type B3 (hereafter *Paramuricea* sp.) that inhabit cold seep and non-seep areas. This species of *Paramuricea* has been the subject of much recent taxonomic work, and was referred to as *Paramuricea* sp. type B3 in most of the references cited here, but falls into the species *Paramuricea* sp. 3 in the most recent analysis (Quattrini et al., 2022). Colonies of *C. delta* were sampled at four sites (MC751, MC885, GC249, and GC234), while *Paramuricea* sp. was only sampled at AT357 (Table S1). Coral colonies were imaged in 2015 at each site/marker using a high-definition digital camera mounted on the ROV. In 2016 and 2017, most coral colonies were revisited and reimaged ($n = 135$ revisited colonies at least once) using the same ROV heading and camera settings, capturing the same image frames to facilitate comparison between years. However, we could not always reimage all colonies due to logistic difficulties. New colonies (and markers) were thus added in 2016 and 2017. A total of 685 images representing 384 colonies were taken, and there were a minimum of three non-seep and seep markers at each site. Imaged colonies were used to investigate the effect of cold seeps on fitness traits of colonies as described below.

2.2.1 | Health status

Coral health of *C. delta* ($n = 401$) and *Paramuricea* sp. ($n = 156$) was assessed visually and classified into four categories as described in Girard et al. (2019); (i) healthy (i.e., live tissue with no visible impact), (ii) unhealthy (i.e., exposed skeleton, excess mucus, or covered in sediment), (iii) colonized (i.e., by hydroid, zoanthid, or mud worms that have a documented negative impact on the colonies), and (iv)

not defined. Each image was digitized using Inkscape 0.48.5 software, by tracing branches of each health category with different sets of color-coded lines. The number of pixels from lines of each category was used to calculate the relative proportions for colony health. Re-imaged colonies in 2016 and 2017 were also digitized and relative proportions of health states were compared between years. The impact of cold seeps on each health category was statistically tested with a generalized linear mixed model (GLMM) using “glmer” function in “lme4” package. Coral species, sites, and seep status were used as fixed effects while colony ID was used as a random effect to account for new/missed colonies over sampling years. GLMM models were also performed on each coral species separately with the same specifications to simplify the model and test for the effect of cold seeps on the health status of coral colonies. Model fit and residuals were visually inspected to check GLMM model assumptions.

2.2.2 | Coral growth rate

Coral growth was measured between consecutive years (2015/2016, 2015/2017, and 2016/2017). Digitized images from 2015 (as explained above) were used as reference templates. Images from 2016 and 2017 were also digitized, classified, and color coded into three categories; (i) old colony (i.e., all observed branches in the previous year), (ii) growth (i.e., new polyps at the terminal end of branches and new branches), and (iii) not defined. The growth proportion of growing or new branches in 2016 and 2017 images was calculated relative to corresponding 2015 templates. Because the number of days between images (i.e., cruises) varied widely among colonies/sites, the growth rate for each colony was normalized to annual continuous growth rate to allow comparisons. The absolute growth rate for each colony was calculated following Equation (1) and the annual continuous growth rate was calculated following Equation (2). AT357 was visited only for two consecutive years (2015 and 2016), while GC249 site was visited only in 2017 and thus, no growth (and regrowth after sampling—see below) data were recorded for these sites.

$$\text{Abs}_{\text{gr}} = \frac{P_{\text{Growth}}}{P_{\text{Old}} + P_{\text{nd}}} \quad (1)$$

$$\text{An}_{\text{gr}} = \frac{\ln(1 + \text{Abs}_{\text{gr}})}{n_{\text{days}}} \times 356.25 \quad (2)$$

where, Abs_{gr} is the absolute growth rate, P_{Growth} is the proportion of the colony in the later image that was new growth since first image, P_{Old} is the proportion of old branches, and P_{nd} is the proportion of not defined category for each colony. An_{gr} is the continuous annual growth rate, while n_{days} is the number of days between taken images.

The effect of cold seeps on growth rate was tested using a generalized linear model (GLM) with a quasi-binomial error distribution to account for overdispersion. The annual continuous growth rate for each coral species was used as a response variable while coral species, seep status, and sites were used as fixed factors.

2.2.3 | Regrowth after sampling

In 2015, branches of *C. delta* ($n = 22$) and *Paramuricea* sp. ($n = 4$) from at least six colonies at each site (except GC249 as stated above) were sampled/clipped for genetic investigation and stable isotopic analysis (see below). Images for each colony were captured before and after sampling in 2015 to calculate the proportion of sampled branches, and the same colonies were reimaged in 2016 and 2017 to measure the potential of colonies to regrow. Like the growth rate calculations, digitized images were color coded, the growth of sampled branches as a proportion of total colony size was calculated, normalized following Equations (1 and 2), and statistically tested using quasi-binomial GLM to assess the effect of cold seeps and site on recovery rate in each coral species.

2.2.4 | Branch loss

The re-imaged colonies in 2016 and 2017 were used to assess branch loss relative to 2015 reference templates of *C. delta* ($n = 55$) and *Paramuricea* sp. ($n = 35$). Images of colonies from 2016 and 2017 were digitized, missing branches were tabulated, and their proportions were calculated relative to the 2015 templates. GLM using a quasi-binomial error distribution was used to test the effect of cold seeps on branch loss and how this differed between sites and coral species.

2.2.5 | Associated epifauna

The images were used to assess the diversity and composition of epifaunal communities associated with *C. delta* and *Paramuricea* sp. colonies. A total of 384 different colonies of *C. delta* ($n = 279$) and *Paramuricea* sp. ($n = 105$) were visually assessed and associated epifauna were counted and identified to the lowest taxonomical level. Community abundance matrices were transformed ($\sqrt{x + 1}$) and used for downstream analysis. Alpha diversity (absolute richness, Chao1, Inverse Simpson and Shannon) indices were calculated using the “*vegan*” package and the influence of cold seep, site, and year was assessed for each species separately. GLMM in “*lme4*” package was used and colony ID was designated as a random effect. Variation in the community composition of epifauna was tested using a PERMANOVA test (“*adonis*” function) with a Bray–Curtis dissimilarity matrix (9999 permutations) and visualized using non-multidimensional scale (NMDS) via “*metaMDS*” function in the “*vegan*” package.

2.3 | Microbiome sample collection

During ROV surveys, samples of *C. delta* ($n = 88$) and *Paramuricea* sp. ($n = 22$) along with surrounding seawater and sediment were collected from cold seep and non-seep markers at each site (total samples $n = 184$, Table S1). Corals, sediment, and seawater will be referred to as microbiome habitats. Coral fragments were

sampled using coral cutters and each sample was placed in separate temperature-controlled chambers (bioboxes or coral quivers) mounted on the ROV. Sediment samples ($n = 45$) were taken at each site using a push core (6.3 cm diameter, depth to c. 20 cm). Seawater samples ($n = 29$) were taken at each site using 2 L Niskin bottles in 2016 and 2017, however in 2015, ~400 L of seawater was collected in situ ($n = 3$ of 29 samples) using a McLane Large Volume Sampler (McLane Laboratories Inc.). All samples were preserved onboard. Approximately, 1 ml from the top 1 cm of each push core was subsampled for microbiome analysis and snap frozen in liquid nitrogen. Coral fragments used for microbiome analysis were preserved also in liquid nitrogen, except *C. delta* samples from 2015 that were preserved in 100% ethanol. Seawater samples (maximum 2 L each) were filtered through a 0.22 μm cellulose acetate filter (Millepore) at sea, and preserved in liquid nitrogen. For 2015 seawater samples, ~400 L were filtered in situ through large (15 cm diameter) 0.22 μm filters, and the filters were cut into quarters, two of which were preserved in liquid nitrogen for microbiome analysis. All samples were shipped to the Pennsylvania State University and stored immediately in -80°C freezer for later genomic analysis.

2.3.1 | 16S rRNA library preparation

Genomic DNA was extracted from approximately 0.5 g coral tissue and sediment samples using Qiagen DNeasy PowerSoil kits (Qiagen) following the manufacturer's protocol. The seawater filters for 2016 and 2017 samples were extracted using DNeasy PowerWater kits (Qiagen), while the filter subsamples from 2015 ($n = 3$, ~1 cm^2 each) were extracted using DNeasy PowerSoil kits (Qiagen). Genomic DNA was used to amplify the V1 and V2 region of the 16S rRNA gene using universal bacterial primers 27F and 355R attached to Illumina adapters (Rodriguez-Lanetty et al., 2013). PCR amplicons were checked on a 1% agarose gel, and sent to the University of Illinois Chicago, DNA services facility, for 16S rRNA library preparation and sequencing on three separate runs using Illumina Miseq platform. Raw sequence data were analyzed using QIIME2 pipeline (ver2017.11—Bolyen et al., 2019) for quality check, taxonomy, and assignment of amplicon sequence variants (ASVs hereafter) abundance (Supplementary Methods).

2.3.2 | Microbiome data analysis

The abundance table of ASVs was normalized using total sum scaling (i.e., proportions) and used for downstream analysis. Notably, we have uneven sampling effort between species, sites, and years in addition to various batch effects including different (i) sequencing run, (ii) preservation method, (iii) DNA extraction kit, (iv) sampling season, and (v) seawater collection methods. This may influence alpha and beta diversity (see Wang & LêCao, 2019) and therefore, we accounted for those covariates in our data analysis (see Supplementary Methods). The normalized ASV table was used to calculate alpha diversity indices including (i) Chao1

richness estimator, (ii) Inverse Simpson evenness, and (iii) Shannon–Wiener diversity for each sample ($n = 184$) using “*vegan*” package. Differences in bacterial diversity were assessed with a generalized linear mixed model using a Bayesian Markov Chain Monte Carlo algorithm (MCMC-GLMM), as implemented in the “*MCMCglmm*” package (Hadfield, 2010), to account for batch effect in the analysis. The effects of habitat and proximity to cold seeps were tested globally first to simplify the model, and then models were built to test the effect of sites, years, and seep status on each habitat separately. Batch effects were accounted as random variables when needed (for model specifications—see [Supplementary Methods](#)).

Similarly, variation in bacterial community composition (beta diversity) was assessed using a linear decomposition model (LDM) in “*LDM*” package (Hu & Satten, 2019), that accounts for batch effects as covariates. The model was built using the “*ldm*” function with the same fixed and random effects as in MCMC-GLMM, with a Bray–Curtis dissimilarity matrix as the response variable (Hu & Satten, 2019). To further validate the LDM model, we performed a PERMANOVA analysis (using “*adonis*” function) without accounting for batch effects as well as a modified version of PERMANOVA implemented in “*LDM*” package (“*permanovaFL*” function) that can also account for batch effects. A principal coordinate analysis (PCoA) was performed using the Bray–Curtis dissimilarity matrix to visualize the clustering pattern of bacterial communities between habitat, sites, and seepage.

2.3.3 | Indicator species analysis and machine learning

To identify bacteria that may act as indicator taxa and are significantly associated with microbiome habitats, we performed indicator species analysis (ISA) using the “*multipatt*” function in “*Indicspecies*” package (De Cáceres & Legendre, 2009). We also used ISA to identify indicator taxa associated with cold seeps within each habitat separately. Furthermore, machine learning analysis was performed using a random forest (RF) algorithm to predict bacterial taxa that may classify different habitats, sites, and seep status. All samples were used for habitat classification using the “*randomForest*” package (Breiman, 2001) with 1001 decision trees at the ASV level. The same RF parameters were used to predict the taxa that classify cold seeps within each habitat separately. Classification accuracy was assessed using the “Out-Of-Bag” error (OOB) implemented in “*randomForest*” function. The most important ASVs ($n = 15$) were extracted based on Decreasing Accuracy Mean values, and their relative abundance was used to test their correlation with the stable isotopic compositions of carbon and nitrogen (see below) using a linear model in “R.”

2.3.4 | Correlation with environmental variables

The correlation between environmental variables and the microbiome was investigated using canonical corresponding analysis (CCA). The CCA was calculated using the “*cca*” function and

fitted to environmental variables (depth, temperature, oxygen, and salinity) as implemented in the “*vegan*” package after omitting missing data. The goodness of fit was calculated using “*anova.cca*” to assess the significance of correlation with each environmental variable.

2.4 | Host transcriptomic analysis

2.4.1 | RNA isolation and sequencing

Samples of *C. delta* preserved in liquid nitrogen (total $n = 12$) were used to assess host transcriptome response to the proximity to cold seeps. Cold seep and non-seep *C. delta* samples ($n = 3$ each each) from MC751 and MC885 were used for transcriptomic analysis. Total RNA was extracted using a modified Trizol/RNeasy Kit (Qiagen, Inc.) protocol (Burge et al., 2013; Polato et al., 2011). Concentration and integrity of RNA were checked ([Supplementary Methods](#)) and total RNA was sent for mRNA library preparation and sequencing (Illumina HiSeq4000; 150 base pair [bp], paired-end reads) through Novogene Corporation Inc. Raw RNA reads were filtered, trimmed and microbial contamination was removed for gene expression analysis (see [Supplementary Methods](#)).

2.4.2 | Transcriptomic data analyses

To assess expression levels, the filtered and trimmed sequences were mapped and quantified against a de novo transcriptome for *C. delta* from the Gulf of Mexico (DeLeo et al., 2021) using Salmon (Patro et al., 2017) in quasi-mapping mode. Significantly differentially expressed genes (DEGs; adjusted p -value $< .5$, absolute \log_2 -fold change [FC] > 1) in relation to site (MC751 vs. MC885) and proximity to cold seeps (seep vs. non-seep) were carried out using the “*DESeq2*” package in R (Love et al., 2014). DESeq2 also clusters DEGs using Pearson correlations to exhibit similarities in expression patterns across samples. Gene IDs and subsequent gene ontology (GO) of DEGs were acquired through BLAST and UniRef databases. The GO terms associated with DEGs were retrieved from the three GO parent categories: biological processes (BP), cellular component (CC), and molecular function (MF).

2.5 | Stable isotope analysis

Carbon ($\delta^{13}\text{C}$) and nitrogen ($\delta^{15}\text{N}$) stable isotopic values were measured in coral tissues and sediment samples collected during the study period (i.e., 2015–2017, total $n = 145$) to identify carbon and nitrogen sources. Frozen tissue of *C. delta* ($n = 88$), *Paramuricea* sp. ($n = 22$) and sediment samples ($n = 35$) in liquid nitrogen were used. Coral tissues were dried at 47°C for 2 days, and repeatedly acidified with two to five drops of 2 N phosphoric acid to dissolve calcium carbonate completely. Samples were dried

and approximately 2 mg from each dried sample was wrapped in a tin capsule and sent to University of California–Davis for carbon and nitrogen stable isotopic analysis using a PDZ Europa ANCA-GSL elemental analyzer interfaced to a PDZ Europa 20–20 isotope ratio mass spectrometer (Sercon Ltd.). Sediment samples for stable isotope analysis were collected and analyzed by Roger et al., (2021). In brief, samples were acidified with 10% HCl to remove carbonates, rinsed, freeze dried, grounded, and were analyzed at the National High Magnetic Field Laboratory (Florida State University) or at the Duke Environmental Stable Isotope Laboratory (see Rogers et al., 2021). Visual inspection of stable isotope data highlighted few outlier values that were likely due to sample preparation or machine error. Therefore, formal outlier analysis was performed (using “outliers” package and function), and outlier values were removed ($n = 2$, one value for each of $\delta^{13}\text{C}$ and $\delta^{15}\text{N}$) from subsequent analyses. The remaining data ($n = 143$) were used to test the effect of seep status and sites on stable isotope values using GLM.

3 | RESULTS

3.1 | Stable isotopes

Carbon and nitrogen stable isotopes were significantly different between coral species and sediments (glm, $\delta^{13}\text{C}-F = 4.8$, $p = .009$; $\delta^{15}\text{N}-F = 124.5$, $p < .001$ —Figure 1). Stable Isotope values also varied significantly between cold seep and non-seep samples of *C. delta* ($\delta^{13}\text{C}-F = 19.2$, $p < .001$, and $\delta^{15}\text{N}-F = 32.2$, $p < .001$) and sediment ($\delta^{13}\text{C}-F = 14.5$, $p < .001$, $\delta^{15}\text{N}-F = 1.6$, $p = .2$), but not in *Paramuricea* sp. ($\delta^{13}\text{C}-F = 0.003$, $p = .95$; $\delta^{15}\text{N}-F = 0.6$, $p = .4$). Furthermore, $\delta^{13}\text{C}$ and $\delta^{15}\text{N}$ values of *C. delta* varied significantly among sites ($\delta^{13}\text{C}-F = 23$, $p < .001$, and $\delta^{15}\text{N}-F = 87.6$, $p < .001$). Interestingly, the range of $\delta^{13}\text{C}$ (−38.17‰ to −16.2‰ for seep and −26.05‰ to −16.2‰ for non-seep) and $\delta^{15}\text{N}$ (1.9‰–9.9‰ for seep and 7.1‰–10.9‰ for non-seep) values in *C. delta* was high (particularly in seep samples; Figure 1).

3.2 | Coral traits

3.2.1 | Health status

Overall, both coral species appeared healthy at all sites (Figure 2) and those patterns remained stable over space and time (Table S2). *Paramuricea* sp. had fewer impacted branches and had a higher proportion of healthy branches on average ($94.9 \pm 13.5\%$ —mean \pm SD) compared to *C. delta* ($87.9 \pm 15.2\%$ —glm, $z = 1.03$, $p = .3$). Proximity to cold seeps had no effect on the average proportion of healthy branches of *C. delta* (mean_{seep} = $87.8 \pm 13.7\%$ and mean_{non-seep} = $89 \pm 17.4\%$; glm, $z = 0.976$, $p = .3$) and *Paramuricea* sp. (mean_{seep} = $95.4 \pm 10.9\%$ and mean_{non-seep} = $94.5 \pm 15.3\%$; glm, $z = .610$, $p = .5$). Furthermore, the proportion of non-healthy

branches also did not vary significantly between seep and non-seep colonies in *C. delta* (mean = 0.1 for both seep and non-seep, glm, $p > .05$). However, *Paramuricea* sp. had a slightly higher proportion of non-healthy branches in seep areas (mean_{seep} = $0.04 \pm 0.09\%$, mean_{non-seep} = $0.02 \pm 0.05\%$, glm, $z = 2.8$, $p = .004$, see Figure 2). Interestingly, the proportion of healthy tissue per colony of *C. delta* was negatively correlated with isotope values ($\delta^{13}\text{C}$ —adj- $R^2 = -.18$, $p = .002$ and $\delta^{15}\text{N}$ —adj- $R^2 = -.07$, $p = .04$), indicating that coral colonies using seep-derived carbon and nitrogen had healthier tissue. This was not the case for *Paramuricea* sp. colonies where the proportion of healthy tissue was not significantly correlated with cold seep isotope values ($\delta^{13}\text{C}$ —adj- $R^2 = .009$, $p = .3$ and $\delta^{15}\text{N}$ —adj- $R^2 = -.05$, $p = .6$; Figure S1).

3.2.2 | Branch loss

Branch loss varied markedly between species (glm, $F = 42.3$, $p < .001$) where no branch loss was observed in *Paramuricea* sp., while *C. delta* lost an average of $0.12 \pm 0.17\%$ branches per colony over the 3-year period (Figure 2). Notably, neither proximity to cold seep (glm, $F = 0.63$, $p = .4$) nor site (glm, $F = 0.2$, $p = .7$) or their interaction affected branch loss in *C. delta* (Table S2).

3.2.3 | Growth rate

Annual growth rate was significantly higher in *C. delta* ($0.05 \pm 0.06\%$, mean \pm SD) than *Paramuricea* sp. ($0.006 \pm 0.008\%$ —glm, $F = 27.4$, $p < .001$ —Figure 2). The proximity to cold seeps did not influence annual growth rate for either *C. delta* (glm, $F = 0.9$, $p = .3$) or *Paramuricea* sp. (glm, $F = 3.8$, $p = .06$). However, annual growth rate of *C. delta* differed among sites (glm, $F = 4.5$, $p = .01$), driven mainly by a significantly low growth rate at the deepest site (MC885, depth = 622–642m; annual growth rate = $0.037 \pm 0.035\%$; glm, t value = -2.296 , $p = .2$ —see Table S2).

3.2.4 | Regrowth after sampling

The capability of coral to regrow after sampling is an indicator of colony energetic reserves that can be used for recovery from injury. Recovery rate did not vary between species (glm, $df = 24$, $F = 1.5$, $p = .2$) where the annual average regrowth was near zero for both *C. delta* ($n = 22$, $0.005 \pm 0.008\%$) and *Paramuricea* sp. ($n = 4$, $0.0006 \pm 0.0006\%$) suggesting slow recovery over time (Figure 2). Furthermore, proximity to cold seeps did not influence the annual recovery rate in *C. delta* (glm, $F = 0.09$, $p = .7$) and *Paramuricea* sp. (glm, $F = 0.003$, $p = .9$ —Table S2). Neither site (glm, $F = 0.7$, $p = .4$ —Figure 2) nor isotope values ($\delta^{13}\text{C}$: adj- $R^2 = -.07$, $p = .7$; $\delta^{15}\text{N}$: adj- $R^2 = -.09$, $p = .9$) influenced relative regrowth rate of *C. delta* colonies. The results of *Paramuricea* sp. regarding lack of influence of proximity to cold seep on recovery rates are preliminary given the small sample sizes.

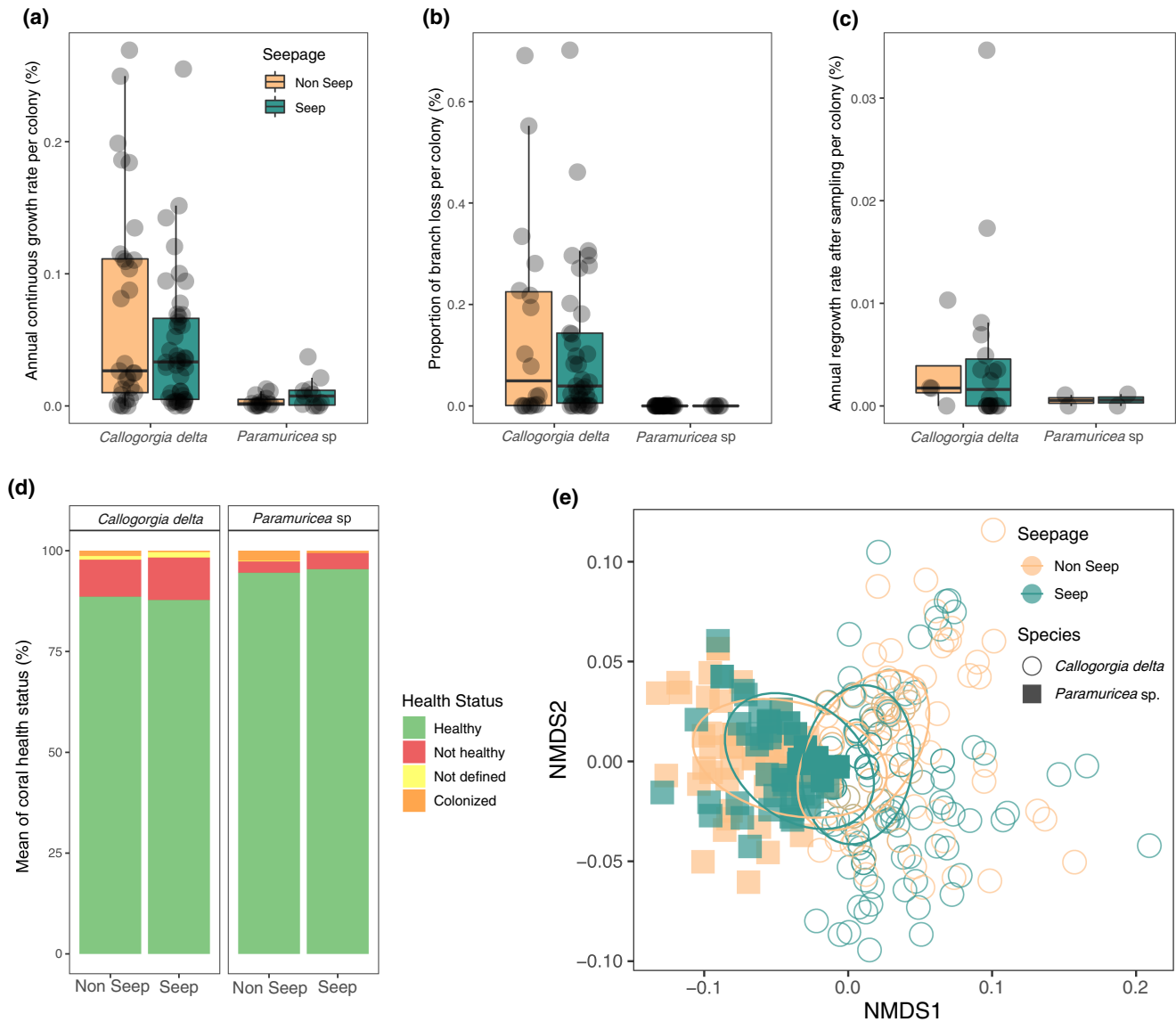


FIGURE 2 Effect of proximity to cold seeps on coral colony traits of *Callogorgia delta* and *Paramuricea* sp. collected from five sites in the Gulf of Mexico. Images of coral colonies were taken in 2015 and then again in 2016 and 2017. Images were digitized, color-coded and rates of colony growth, branch loss, regrowth after sampling and the healthy proportion of corals colonies were calculated and compared between seep and non-seep corals. Boxplots represent coral growth rate (a), branch loss (b), and regrowth after sampling (c) per colony, while stacked bar plot shows the average proportion of each health category in coral colonies (d). Coral growth rate and branch loss varied significantly between *C. delta* and *Paramuricea* sp., although the proximity to cold seeps did not impact any of the measured coral traits in either coral species, except the proportion of non-healthy branches in *Paramuricea* sp. Furthermore, epifauna associated with coral colonies were counted and identified to the lowest taxonomical unit. Non-multidimensional scale (NMDS) showed distinct epifaunal communities between coral species (e). The proximity of cold seeps had significant, but limited (1% of variation), influence on the epifaunal communities in *C. delta*, but not in *Paramuricea* sp. colonies.

3.2.5 | Associated epifauna

Each coral species harbored a distinct epifaunal community with little overlap between species. Colonies of *C. delta* were associated with 23 taxa dominated by ophiuroid sp1 (52.4%), cat shark eggs (22%), an unknown gastropod (12.7%), and *Eumunida picta* (2.4%; Figure S2). *Paramuricea* sp. was associated with only eight epifaunal taxa including; two ophiuroid species (52.7% and 18.8%), a crab (14.6%), an aplousobranch (8.9%), and an anemone (2.3%; Figure S2). The diversity of the epifauna (i.e., absolute richness,

Chao1, Inverse Simpson, and Shannon-Wiener indices) did not change with proximity to seepage, site, or year in either coral species (Table S3). In contrast, the composition of the epifaunal community varied significantly between coral species (PERMANOVA, $R^2 = .29$, $p < .001$ —Figure 2). The epifauna associated with *C. delta* were primarily influenced by site (PERMANOVA, $R^2 = .14$, $p < .001$), while proximity to seepage ($R^2 = .01$, $p < .001$) and year ($R^2 = .0097$, $p = .0095$) had significant, but limited, effects as they explained only 1% each of the variation. *Paramuricea* sp. associated communities were not influenced by either year ($R^2 = .01$, $p = .1$) or proximity

to seepage ($R^2 = .008$, $p = .2$) nor their interactions ($R^2 = .006$, $p = .3$ —Table S4).

3.3 | Microbiome community

3.3.1 | Taxonomic profile

The taxonomic profile of bacterial communities varied markedly among corals and surrounding seawater and sediment (Figure 3). The bacterial community of *C. delta* was dominated by *Mollicutes* ($75.5 \pm 28.7\%$ mean \pm SD), unclassified bacteria ($8.7 \pm 15.9\%$), and Epsilon-proteobacteria ($4.7 \pm 11.7\%$), and two ASVs of *Endozoicomonas* (1.4%) that, combined, comprised 92.3% of relative microbial abundance of *C. delta*. *Paramuricea* sp. was dominated by SUP05 bacteria ($38.6 \pm 24.6\%$), *Endozoicomonas* ($29.8 \pm 17.9\%$), and *Candidatus Xenohaliotis* ($10.2 \pm 11.8\%$) that, combined, comprised 81.3% of relative microbial taxa abundance. In contrast, seawater and sediment were not dominated by certain taxa, and the majority of ASVs were rare (i.e., less than 1% of relative abundance—Figure 3).

3.3.2 | Alpha diversity

The bacterial diversity differed primarily among habitats: coral species, surrounding seawater, and sediment (Figure 3). Bacterial richness (Chao1), evenness (inverse Simpson), and biodiversity (Shannon) were significantly higher in sediment and seawater than *C. delta* and *Paramuricea* sp. (MCMCglmm, pMCMC < 0.001 , Table S5). Proximity to cold seeps had no effect on bacterial diversity indices in coral species or the seawater samples (pMCMC > 0.05), unlike sediment where bacterial richness and evenness changed significantly between seep and non-seep samples (pMCMC < 0.047 and 0.02 , respectively—Table S5). Repeated analysis with different statistical model (GLM) similarly failed to detect an effect of seepage on coral or seawater associated bacterial diversity except in sediment samples (Tables S5 and S6). Furthermore, spatial (particularly in the most active seep site GC249, pMCMC < 0.01) and temporal (pMCMC < 0.01) variation was noted in *C. delta* and sediment bacterial communities, but not in *Paramuricea* sp. and seawater (Table S6).

3.3.3 | Beta diversity

Bacterial community composition differed among corals and surrounding seawater and sediment (LDM, variance explained [VE] = 60.6%, $p < .01$ —Figure 3). Proximity to cold seeps did not change bacterial composition in *C. delta*, *Paramuricea* sp., or seawater samples. Composition of bacterial communities in sediments varied with proximity to seepage (LDM, VE = 2.4%, $p < .01$ —Figure S3), but no temporal variation (LDM, VE = 1.04%, $p = .7$) was observed

suggesting stability of the bacterial community in the sediment over time. Repeating the analysis with different models (see methods) indicated that bacterial community composition of *C. delta* (PERMANOVA, $F = 3.4$, $R^2 = .3$, $p = .02$ —PERMANOVA-FL, $F = 1$, $p = .04$) and, again, sediment (PERMANOVA, $F = 2.6$, $R^2 = .04$, $p = .03$ —PERMANOVA-FL, $F = 0.6$, $p = .006$) varied significantly with proximity to seepage. Seepage did not affect bacterial composition in *Paramuricea* sp. and seawater samples (Table S7).

To avoid data noise and further explore the variation of microbiome communities associated with *C. delta* near and far from seeps, we compared *C. delta* colonies collected from the most active seep site, GC249 ($n = 8$) to colonies growing at a site with non-seep indicators, GC234 ($n = 8$). GC249 had a strong chemosynthetic signature and colonies were growing next to an oily mussel bed with significantly different stable isotope values compared to all other sites (glm, $\delta^{13}\text{C}$ — t -value = -7.668 , $p < .001$, and $\delta^{15}\text{N}$ — t -value = -3.851 , $p < .001$ —see Table S8A; Figure S4), whereas GC234 had no signs of any seepage. We found that the microbiome composition of *C. delta* colonies was significantly different between these seep and non-seep sites, explaining 34.4% of the microbiome variation between them (LDM, VE = 34.4%, $p < .01$ —PERMANOVA-FL, $F = 6.7$, $p = .02$; Table S8B). Notably, LDM identified two ASVs (SUP05 and *Methylobacterium*) that were differentially abundant between seep and non-seep colonies. This large change in bacterial community composition was not accompanied by a change in the diversity of the microbiome of *C. delta* (GLM, global $p > .5$), despite the notable differences in coral tissue stable isotope values at these sites.

3.3.4 | Indicator species analysis

Indicator species analysis (ISA) identified only 23 indicator taxa for cold seeps for all samples collected from corals, sediment, and seawater combined; five of them were SUP05 phylotypes. There were approximately 19 times more taxa indicating non-seep sites ($n = 431$ taxa; Table S9). Indicator taxa for each coral species separately were fewer in number; two SUP05 were indicators for *C. delta* and a single SUP05 was an indicator for *Paramuricea* sp. Furthermore, ISA between GC234 and GC249 identified a SUP05 as the sole indicator taxon for seep colonies (this was one of the two SUP05 indicators found with all *C. delta* colonies—see above). Interestingly, the relative abundance of this indicator SUP05 varied significantly between seep and non-seep colonies (ANOVA, $F = 8.7$, $p = .01$ —Figure 4). Also, the relative abundance of SUP05 had a strong negative correlation with carbon (lm, $\text{adj-}R^2 = -.64$, $p < .001$) and nitrogen (lm, $\text{adj-}R^2 = -.38$, $p < .001$) isotope values, highlighting the potential role of SUP05 in cold seep habitats (Figure 4). Notably, the relative abundance of the dominant SUP05 phylotype associated with *Paramuricea* sp. also varied significantly between seep and non-seep colonies and was negatively correlated with carbon and nitrogen stable isotope values, however, this was not detected by indicator species analysis (Figure S5). Seawater samples had 11 bacterial indicator taxa for cold seeps (mostly SAR11

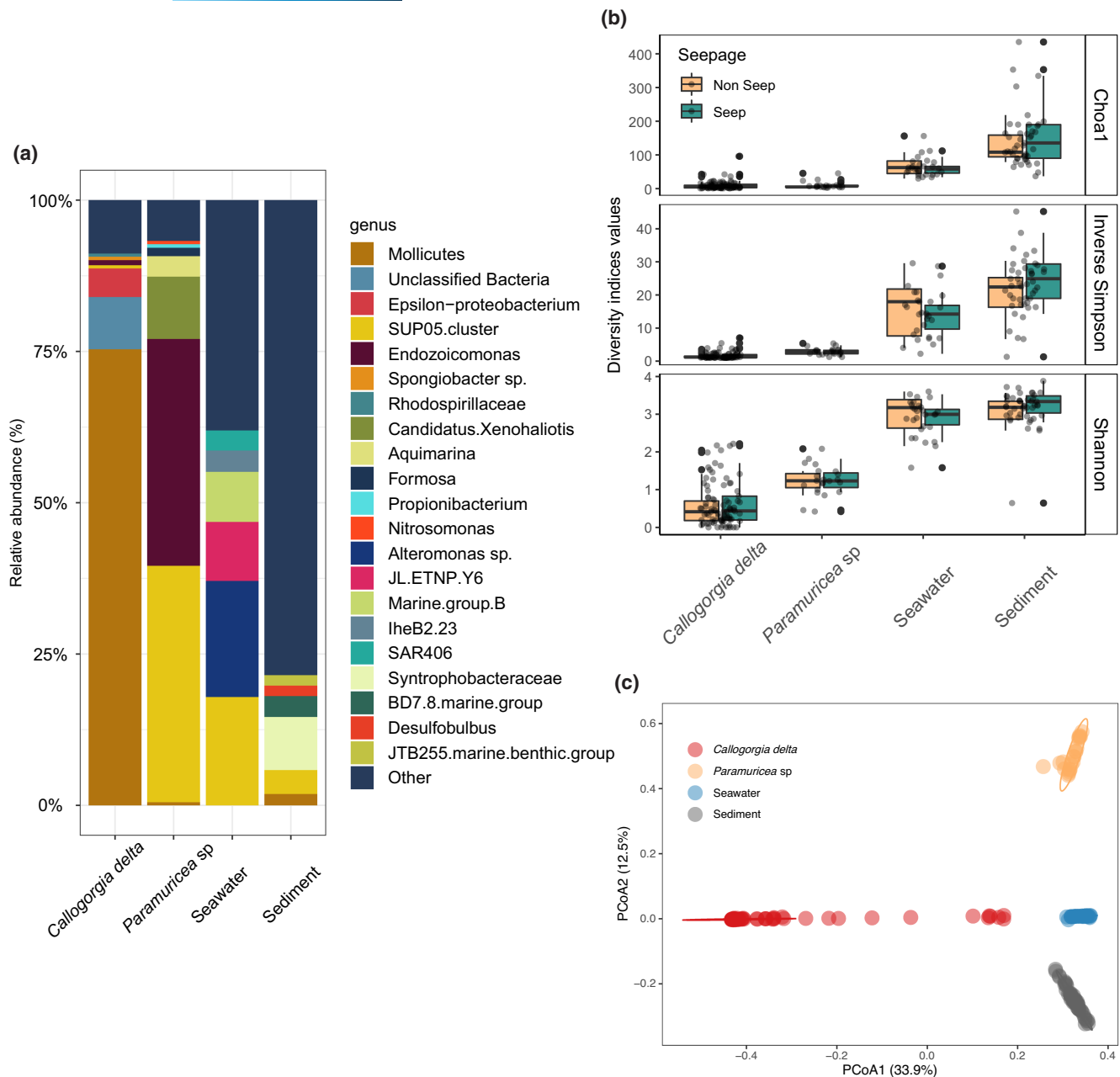


FIGURE 3 Diversity and composition of microbiome communities associated with *Callogorgia delta*, *Paramuricea sp.* and surrounding seawater and sediment ($n = 184$), collected from cold seep and non-seep at five sites in the Gulf of Mexico. Bar plot shows taxonomic profile of microbiome community (a) where each coral species had distinct taxa relative to surrounding seawater and sediment. Alpha diversity of microbiome community is represented as box plots (b) and demonstrates that Chao1, Inverse Simpson, and Shannon–Wiener indices varied markedly between corals, sediment, and seawater, while proximity to cold seep had no effect on corals and seawater except only the sediment microbiome. Similarly, principle coordinate analysis (c) showed that each of the habitats had a unique microbiome community while the proximity to cold seeps did not change the composition.

clade), while as many as 84 taxa indicated proximity to seepage in sediment samples, most of them are known as seep-associated bacteria (e.g., *Desulfobulbus*, *Desulfobulbaceae*, *Sulfurovum*, Methylophilic group, *Sulfurimonas*) with slight differences between sites. Differences between sites with respect to indicator taxa were evident in *C. delta* where site was indicated by five *Shewanella sp.* at GC234, a single SUP05 at MC885, and Epsilon-proteobacteria and unidentified Oceanospirillales (the family of SUP05) at MC751.

3.3.5 | Random forest analysis

Random forest analysis demonstrated that habitat (coral species, seawater, sediment), but not proximity to seepage, was the best classifier for all samples (“Out of Bag” error, OBB = zero). Top taxa that classified habitats were *Mollicutes*, several *Endozoicomonas* phylotypes, Epsilon-proteobacteria, and SUP05, all of them were the dominant ASVs that reported to be associated with corals,

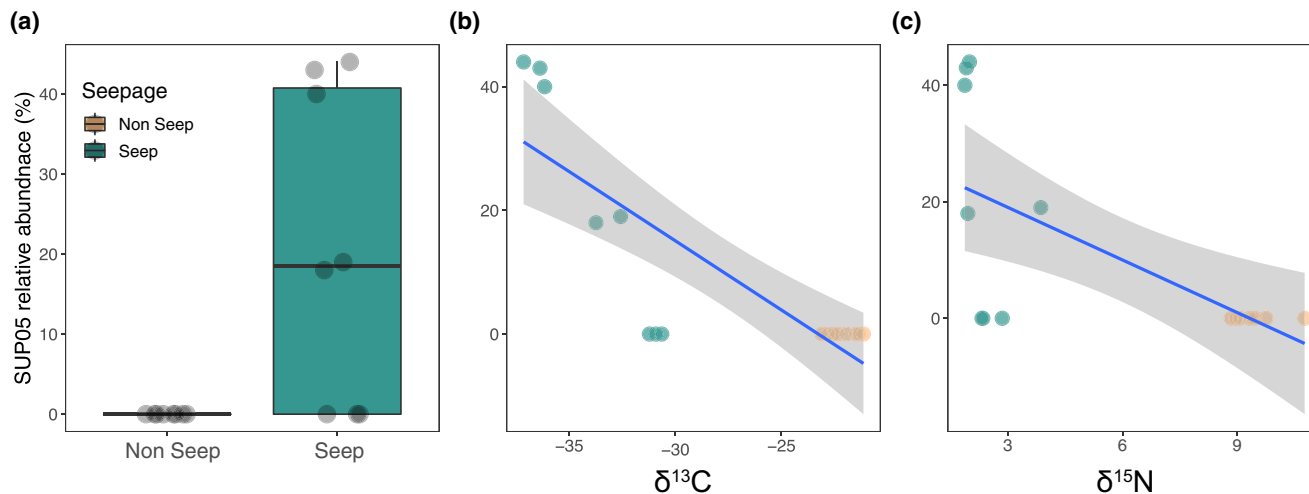


FIGURE 4 Analysis of SUP05 phylotype associated with *Callogorgia delta* colonies collected from the most active seep site (GC249) and a non-seep site (GC234). This SUP05 phylotype was reported as an indicator taxon and a differentially abundant taxon (by LDM), for *C. delta* colonies collected at GC249 versus GC234, as well as it was the indicator taxon for all seep *C. delta* colonies collected from different sites. (a) Box plot demonstrates the significant variation in relative abundance of the SUP05 between seep and non-seep colonies. Point plots show the correlation between (b) carbon and (c) nitrogen stable isotope values and the relative abundance of the SUP05 phylotype in seep and non-seep colonies. The correlation was strongly negative for both carbon and nitrogen stable isotopes suggesting upregulation of relative abundance of SUP05 in seep colonies. As such, SUP05 likely facilitate utilization of seepage reduced chemicals.

seawater, and sediments (see Figure 3). When proximity to seepage was used as the classifier, samples of *C. delta* (OOB = 34.1%), *Paramuricea* sp. (OBB = 31.8%), seawater (OOB = 48.3%) and sediment (OOB = 33.3%) were often mis-assigned, highlighting the relative similarity of microbial communities across seep versus non-seep samples within species compared to the differences between corals, seawater, and sediment. In contrast, RF successfully classified *C. delta* colonies from GC234 versus GC249 according to their seep origin with 87.5% accuracy (OBB = 12.5%). The differentially abundant *Methylobacterium* and the indicator SUP05 phylotype that previously identified in LDM and ISA (see above) were among the top classifier ASVs, in addition to other ASVs (e.g., two unidentified bacteria, Epsilon-proteobacterium, several *Shewanella*, and *Endozoicomonas*). Furthermore, when habitats were classified separately, “site” and “year” classifiers assigned bacterial samples with >80% accuracy (OOB <20%) except in sediment samples where the bacterial community was stable across years (OOB 48.9%).

3.3.6 | Correlation with environmental variables

Canonical correspondence analysis (CCA) on bacterial communities derived from corals and surrounding seawater and sediment with environmental variables explained 13% of bacterial variation while 87% of bacterial variation remained unexplained. CCA revealed significant correlation between bacterial composition and depth (ANOVA, $F = 4.8774$, $p < .001$), but not with temperature ($7 \pm 1.8^\circ\text{C}$), oxygen ($187 \pm 41 \mu\text{g L}^{-1}$), or salinity ($35 \pm 0.06\%$) which had only minor variation among sites.

3.4 | Host gene expression

A total of 27,927 genes were recovered from *C. delta* colonies ($n = 12$) sampled from seep and non-seep colonies at two sites, while filtering out low abundance genes reduced this set to 15,420 genes. Principle component analysis failed to cluster host transcriptomes by site or proximity to seepage (Figure 5). Differential gene expression (DGE) between seeps was relatively low where only 11 genes were upregulated ($\log_2\text{-FC}$; range: 2.7–6.5, mean = 4.2) and 10 genes were downregulated (FC, range: 1.8–6.6, mean 3.6) between cold seep versus non-seep samples (Figure 5). Out of 21 up/downregulated genes, nine were uncharacterized proteins while the remaining 12 genes were housekeeping genes (Table S10). The GO for under-expressed genes included integral component of membrane, nucleic acid binding, ATP binding, collagen-containing extracellular matrix, nitrogen compound metabolic process, while the GO for the over-expressed genes included protein dimerization activity, DNA binding, regulation of transcription by RNA polymerase II, nucleic acid binding, and DNA integration (Table S11).

In contrast, site had a noticeable effect on host transcriptomes where 113 genes had higher expression levels at MC751 (FC; 1.3–5.5, mean = 3.1) and 18 genes had higher expression at MC885 (FC; 1.5–4.25, mean = 2.7; Table S12). Out of the 121 DEGs among sites, 48 genes were uncharacterized proteins. The over-expressed genes ($n = 113$) at MC751 yielded GO terms including G protein-coupled receptor activity, protein tyrosine phosphate activity, ATP binding, and DNA replication (Table S13). Whereas the 18 DEGs at MC885 aligned with GO terms related to DNA binding, integral component of membrane, metal ion binding, ATP binding, intercellular protein transport,

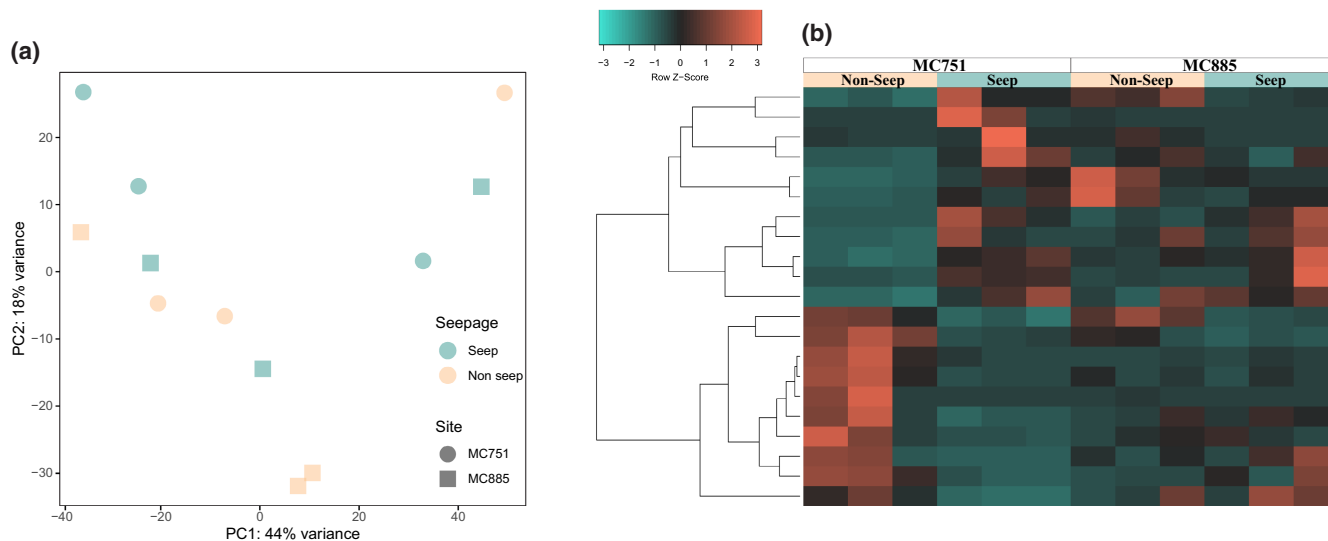


FIGURE 5 Host transcriptome analysis of *Callogorgia delta* collected from cold seep and non-seep markers ($n = 3$ each) at two sites (MC751 and MC885, total $n = 12$) in the Gulf of Mexico. a) Principle coordinate analysis of *C. delta* gene expression failed to cluster samples by either site or proximity to cold seeps. b) Nevertheless, differential gene expression of *C. delta* in response to proximity to cold seep was evident in the heatmap. Genes are hierarchically clustered based on Pearson's correlations of expression across samples and differential gene expression was considered significant if adjusted p -values (false discovery rate) $<.05$ and absolute \log_2 -fold change was >1 . Rows are individual genes and columns are individual samples and colors indicates the row z score. Heatmap show 21 genes differentially expressed genes relative to their proximity to cold seepage (seep vs. non-seep).

and actin cytoskeleton organization. Analysis of DEGs within each site separately revealed 213 and 26 DEGs relative to seepage at MC885 and MC751, respectively, none of them were associated with detoxification or sulfur oxidation pathways (Table S13). Notably, a single housekeeping gene (fosB-like protein) exhibited higher expression near seeps compared to away from seeps at both sites.

4 | DISCUSSION

Cold-water corals are a diverse group that can be found from shallow water to over 2000m depth. Some of the habitats they occupy represent unique challenges such as cold seeps that release hydrocarbons-rich fluid which can be toxic to many organisms. However, seepage effluents can fuel food chains via chemosynthesis when chemical concentrations are high enough (Åström et al., 2018; Childress et al., 1986). Previous stable isotope analyses showed that corals living near seeps feed mostly on photosynthetically derived suspended organic matter and plankton and failed to detect significant input from chemosynthetic sources (Becker et al., 2009). It was thought that corals may be a later successional stage that colonize carbonate outcrops after most surface expression of seepage has subsided, and thus, corals occupy seep habitats primarily to take advantage of the available carbonate substrate (Cordes et al., 2008; Fisher et al., 2007; Xu et al., 2019). Here, colonies of two coral species, *Callogorgia delta* and *Paramuricea* sp. type B3, were observed living close to and on top of chemosynthetic organisms that rely primarily on active seepage. Hence, we investigated whether colonies of these two coral species gained benefits or, possibly, incurred a cost when living near cold seeps in the deep Gulf of Mexico. We

provide the first evidence that both coral species obtain some nutrition in situ from chemosynthetic primary production at active seeps, but in a species-specific manner. Proximity to active signs of seepage was accompanied by shifts in microbiome community composition in *C. delta* and an increase in the relative abundance of SUPO5 phylotypes in both coral species. We thus suggest that changes in their microbial symbiont communities provide a mechanism for corals to survive and grow near active cold seeps.

4.1 | Proximity to cold seeps affects diet of *C. delta* and *Paramuricea* sp. in different ways

We report here that stable isotopes from *C. delta* colonies sampled at cold seeps were significantly lower in $\delta^{13}\text{C}$ and $\delta^{15}\text{N}$ than colonies sampled far from seeps indicating a component of chemosynthetically derived food in their diet (see Figure 1). Furthermore, the proportion of live tissue on *C. delta* colonies was correlated with chemosynthetic-derived $\delta^{13}\text{C}$ and $\delta^{15}\text{N}$ values suggesting that *C. delta* colonies benefited from ingesting chemosynthetically fixed carbon (Figure S1). This contrasts with most previous studies where stable isotope values did not indicate chemosynthetic food input for coral species collected in situ, including fossil coral samples (e.g., Deng et al., 2019; Xu et al., 2019).

Here, we suggest that *C. delta* likely obtained chemosynthetic food primarily via heterotrophic filter feeding, as previously proposed (Becker et al., 2009). This is because the majority of investigated *C. delta* colonies near seeps had both chemosynthetic and photosynthetic stable isotope values (Figure 1) highlighting the flexibility of *C. delta* to obtain food from different sources. The alternative explanation, that

C. delta was supplemented with chemosynthetically fixed carbon from a bacterial symbiont living within its tissue, was less likely for three reasons. (i) The assembled whole genome of Mollicutes (i.e., the dominant bacterial phylotype, see Figure 3) collected from some of the *C. delta* colonies used in the current study showed lack of chemosynthetic pathways (Vohsen et al., 2022). (ii) The relative abundances of *C. delta* dominant symbiotic bacteria (i.e., Mollicutes—Figure 3) were not significantly different between seep and non-seep samples and did not correlate with stable isotope values (Figure S6). (iii) Few colonies had low relative abundance of SUP05 in GC249 despite a strong chemosynthetic signature in their tissue (Figure 4). Thus, it is unlikely that SUP05 is the primary source of the pronounced chemosynthetic signature in most of *C. delta* colonies near active seeps. SUP05, instead, may partially supplement the diet for some colonies or contribute to detoxifying seep effluents (see below).

In contrast, stable isotope values in *Paramuricea* sp. colonies were similar in seep and non-seep colonies. The difference in stable isotope values between *C. delta* and *Paramuricea* sp. may be attributed to their; (i) feeding strategies and prey size, (ii) assimilation/storage efficiencies, and/or (iii) metabolic pathways of coral hosts and/or associated bacteria to digest chemosynthetically derived food. Vohsen et al. (2020) proposed that the dominant endosymbiotic sulfur-oxidizing bacteria (SUP05) found in some of our samples (see Figure 3a) supplement the diet of *Paramuricea* sp. despite slightly similar stable isotope values between seep and non-seep colonies (see also Figure 1). They inferred this from; (i) the negative correlation between the relative abundance of SUP05 and isotopic composition of carbon and nitrogen, and (ii) active transcription of genes related to chemosynthetic pathways. Here, we also reported that the relative proportion of SUP05 was significantly higher in cold seep *Paramuricea* sp. colonies than in non-seep colonies (Figure S5). This suggests that *Paramuricea* sp., similar to *C. delta*, may upregulate abundances of SUP05 symbionts near active cold seeps that provide some chemosynthetically derived nutrition for the host. As such, *Paramuricea* sp. likely obtains part of its nutrition chemoautotrophically when living near active cold seeps while otherwise relying on heterotrophic filter feeding. However, *C. delta* appears to primarily feed heterotrophically where chemosynthetic food is available to be directly consumed and thus, it has lower (chemosynthetic) isotopic values near seeps compared to *Paramuricea* sp. Thus, both species behave like a mixotroph but to a different extent. We concluded that both coral species opportunistically use available food and substrate near cold seeps, however, each species obtains their chemosynthetic food using a different approach.

4.2 | Variability of microbiome communities between seep and non-seep coral colonies

Changes in microbiome communities have been observed in shallow and deep-sea corals as a response to environmental gradients (Osman et al., 2020; van de Water et al., 2017). Here, we found significant, but subtle (2%), variation in the composition of microbial communities between seep and non-seep colonies of *C. delta*. The difference

is more pronounced when the most active seep site was compared to the non-seep site (variance explained 37%). Hence, there might be a link between seepage chemical composition and concentration on the microbial communities of *C. delta*. Furthermore, the influence of seepage on the corals' microbiome might be also due to having to digest a chemosynthetically derived diet near active seeps rather than photosynthetic-derived organic carbon far from active seeps (Figure 1). Starved deep-sea corals, *Lophelia pertusa* and *Madrepora oculata*, fed on various types of diets exhibited diet specific changes in their microbiome (Galand et al., 2020), suggesting that diet may drive, or at least contribute, to the change in microbial composition. However, the microbiome of *L. pertusa* has also been shown to be far more variable than that of *M. oculata*, suggesting that it has more flexibility in the potential niches it could occupy (Meistertzheim et al., 2016). Overall, shifts in microbial composition might be a key adaptive mechanism of corals that facilitate survival of colonies near cold seeps and other habitats.

Microbiome-host specificity and composition in corals relative to surrounding seawater and sediment are well-documented patterns for shallow and deep-sea coral species (La Rivière et al., 2015; Osman et al., 2020). This specificity may be linked to several factors such as the chemical composition of coral mucus, the transmission mode of the microbiome, or host-bacteria recognition mechanisms (Osman & Weinnig, 2022; van de Water et al., 2018). However, biogeographical variation between sampling sites may be also attributed to host specificity where *Paramuricea* sp. was exclusively sampled at AT357 at 1140–1160m, while *C. delta* was sampled at the remaining four sites at 450–800m. Our data support this notion that depth was significantly correlated with microbiome composition (e.g., Franco et al., 2020), unlike other environmental variables (temperature, salinity, and oxygen) that did not change microbiome composition of either species. Notably, depth was confounded with sites which was likely driving the difference in microbiome composition (see Table S7).

Interestingly, SUP05 phylotypes were associated with both coral species, had a strong correlation with carbon and nitrogen stable isotope values, and their relative abundance varied with exposure to active seepage. SUP05 are common sulfur-oxidizing endosymbionts associated with a broad range of fauna in cold seep habitats (see Morris & Spietz, 2022). Previously, it was proposed that the lack of specialized respiratory structures or oxygen-transport mechanisms in cnidarians would preclude corals from harboring sufficient chemosynthetic symbionts to supply the majority of their nutrition because they would not be able to satisfy the high oxygen demand of chemosymbionts (Childress & Girguis, 2011). However, SUP05 was recently found associated with *Paramuricea* sp. in cold seep habitats, transcribing genes related to carbon fixation and sulfur oxidation processes (Vohsen et al., 2020). Similar symbiosis between SUP05 and sea anemones (*Ostiactis pearseae*) living near active hydrothermal vents (3700m) was also discovered in the Gulf of California (Goffredi et al., 2021). This suggests that there is a mechanism to deliver adequate oxygen to maintain a symbiotic relationship between SUP05 populations

and cnidarian hosts sufficient to contribute to the host nutritional needs. It is worth noting that even a relatively small contribution to bulk nutrition can be critical to the hosts in nutrient limited habitats or if the contribution includes essential nutrients not otherwise available. Our work supports the hypothesis that SUP05 phylotypes are functional chemosymbionts in corals near active cold seeps, and may provide supplemental nutrition to the host. Furthermore, several *Endozoicomonas* phylotypes were dominant in both coral species. *Endozoicomonas* is a wide-spread coral associate enriched in genes related to carbon sugar transport and utilization (Neave et al., 2016). *Endozoicomonas* also were reported in two cold-water coral species that live below 1000m emphasizing the potential role of *Endozoicomonas* as endosymbionts of deep-sea corals (Kellogg & Pratte, 2021).

4.3 | Proximity to cold seeps does not change colony phenotypes or host transcriptome

We measured a comprehensive set of holobiont phenotypes in relation to proximity to cold seeps to explore whether living near cold seep provide benefits or incurs a fitness cost for the coral colonies. This study assessed 685 images of 384 colonies (to quantify colony traits) and 184 biological samples of coral tissue, surrounding sediment and seawater collected at five sites over 3 years, which represent a substantial sampling effort with the power to detect the effects of cold seeps on coral colonies.

4.3.1 | Colony phenotypes

Our data showed a correlation between apparent healthy tissue of *C. delta* colonies and chemosynthetic isotope values of carbon and nitrogen highlighting that colonies gain benefits from feeding on chemosynthetic-derived food. However, annual growth and recovery from sampling rates were relatively low in both *C. delta* and *Paramuricea* sp. despite the proximity to cold seeps. This was in line with Girard et al. (2019) who estimated the growth rate of *Paramuricea biscaya* and *Paramuricea* sp. B3 in the Gulf of Mexico to be only 0.14–2.5 cm/year/colony. These corals grow very slowly indeed, and it is therefore unsurprising that we could not detect a temporal effect of seepage on these traits over the course of 3 years. Notably, the proportion of branch loss in *C. delta* was higher than *Paramuricea* sp., while the proportion of non-healthy branches was higher in *Paramuricea* sp. colonies at seeps, highlighting the susceptibility of both coral species to environmental impact or biotic interactions (predations and physical damage).

Epifauna of *C. delta* and *Paramuricea* sp. species were host specific. Cordes et al. (2008) similarly reported distinct epifaunal communities associated with *Lophelia pertusa* relative to those associated with vestimentiferan tubeworm aggregations that occur nearby at the same sites. They suggested that habitat heterogeneity, the specific niche provided by each host, and different

interactions with the host species contributed to this variation. The host specificity in our study may also be related to biogeographic distance between *C. delta* and *Paramuricea* sp. sampling sites which do not overlap in depth. Proximity to cold seeps had a significant, but limited, effect on associated fauna as it explained only 1% of the variation. This may be attributed to (i) the mobile nature of epifauna associated with both coral species that were dominated by ophiuroids, gastropods, crabs, and other crustaceans (Figure S2), (ii) the higher diversity of fauna associated with cold seep habitats (due to food availability) relative to background sediment.

Ophiuroids were the dominant epifaunal group on both coral species (brittle stars—Figure S2), a general pattern for cold-water coral species world-wide (Mosher & Watling, 2009). In our study, proximity to cold seeps did not have a significant effect on relative abundance of brittle stars in *Paramuricea* sp. (glm, $F = 0.5$, $p = .4$), but their relative abundances were significantly higher in cold seep than non-seep colonies of *C. delta* (glm, $F = 28$, $p < .001$). Although the presence of ophiuroids has been shown to limit impacts of acute exposure to hydrocarbons (Girard et al., 2016), it seems unlikely that brittle stars offer significant physical protection of colonies from diffuse seep effluents. The variation is more likely attributed to food availability in seep habitats or colony sizes as larger colonies provide space for higher numbers of brittle stars.

4.3.2 | Host gene expression

Callogorgia delta has a documented affinity for living around areas of active hydrocarbon seepage in the Gulf of Mexico (Quattrini et al., 2013). However, we could not detect a noteworthy difference in the global gene expression patterns between seep and non-seep colonies (Figure 5). In contrast, the comparison between sites (MC751 and MC885) showed a larger number of DEGs (Table S12), but the subsequent GO identifications indicated that these genes were related to typical housekeeping processes (Table S13). As such, *C. delta* does not primarily rely on regulation of a suite of specific genes within the coral transcriptome to augment tolerating active cold seep exposure in the Gulf of Mexico.

The absence of detectable differences in host gene expression between seep and non-seep colonies may be attributed to lack of power to detect a variation in gene expression. We used three colonies from seep and non-seep markers at each site to detect the variation in gene expression. More sampling effort is needed, particularly between active seep and non-seep sites, to understand the response of host to seep exposure. The reported slight differences in gene expression profiles in our study could be explained, at least partially, by temporal cycles that the corals experience. Research on shallow-water corals has suggested the expression patterns of corals can change throughout tidal and lunar cycles (Oldach et al., 2017; Ruiz-Jones & Palumbi, 2017). Since the corals for this study were sampled across three different years and seasons, it is possible that natural rhythms influenced gene expression patterns.

5 | CONCLUSION

This study showed that *C. delta* and *Paramuricea* sp. type B3 populations living near signs of active cold seeps gain benefits from seepage including input of chemosynthetic-derived nutrition, but this pattern was species specific. Each coral species may have used a different mixotrophic strategy to obtain chemosynthetically produced food, either via direct uptake from the environment or through a symbiotic relationship with sulfur-oxidizing bacteria as suggested by Goffredi et al. (2021) and Vohsen et al. (2020). Therefore, we propose that these coral populations do not simply benefit from the substrate at seeps as previously hypothesized but may also benefit from additional sources of nutrition in seep habitats. Interestingly, the proximity to cold seeps significantly affected the microbiome communities in *C. delta* and the relative abundance of various SUP05 phylotypes in both coral species were upregulated that likely facilitated corals to utilize or adapt to cold seeps. In contrast, fitness traits of coral colonies or host genes related to detoxification/sulfur pathways were not affected suggesting that living near cold seeps does not impose a cost we could detect in these coral species. Our study provides the first evidence that corals utilize available chemosynthetically derived food in cold seep habitats with aid of their associated microbiome communities.

AUTHOR CONTRIBUTIONS

Iliana B. Baums, Charles R. Fisher, and Erik Cordes acquired funding, designed the survey, and lead the field work. Samuel A. Vohsen, Fanny Girard, and Alexis M. Weinnig additionally conducted field work. Samuel A. Vohsen and Kaitlin E. Anderson conducted all laboratory work involving stable isotopes of coral tissue and 16S sequencing. Fanny Girard, Rafaelina Cruz, Orli Glickman, Lena M. Bullock, and Kaitlin E. Anderson performed image digitization, while Alexis M. Weinnig performed transcriptomics laboratory work and analysis. Eslam O. Osman conducted the data analysis, prepared visualizations, and wrote the first draft that was edited and approved by all authors.

ACKNOWLEDGMENTS

The authors thank ECOGIG for the funding. Special thanks to Kelsey Rogers and Jeff Chanton for providing stable isotope data of sediments. The authors also thank the operation team of EV Nautilus and ROV Hercules, Ocean Inspector, and ROV Global Explorer. This is contribution no. 598 from ECOGIG consortium.

FUNDING INFORMATION

This work was primarily funded by Ecosystem Impacts of Oil and Gas Inputs to the Gulf (ECOGIG) consortium through the Gulf of Mexico Research Initiative (GOMRI) provided to professors Iliana B. Baums, Erik Cordes, Charles R. Fisher.

CONFLICT OF INTEREST

The authors declare that they have no conflict of interest.

DATA AVAILABILITY STATEMENT

Raw sequences of 16S rRNA and transcriptome were deposited to NCBI Bio-project number PRJNA773229. Coral images, raw and processed tables were deposited to The Gulf of Mexico Research Initiative Information and Data Cooperative—GRIIDC (2015; <https://doi.org/10.7266/N7CF9NH9>—2016 and 2017; <https://doi.org/10.7266/8a2xrm9k>). R scripts and Markdown documents are available on GitHub platform; <https://github.com/Eslam-Osman/Deep-Sea-Microbiome>. All data are publicly available.

ORCID

Eslam O. Osman  <https://orcid.org/0000-0002-5517-8186>
 Samuel A. Vohsen  <https://orcid.org/0000-0003-1710-292X>
 Fanny Girard  <https://orcid.org/0000-0002-7846-2710>
 Alexis M. Weinnig  <https://orcid.org/0000-0001-8858-4837>
 Erik Cordes  <https://orcid.org/0000-0002-6989-2348>
 Iliana B. Baums  <https://orcid.org/0000-0001-6463-7308>

REFERENCES

- Åström, E. K. L., Carroll, M. L., Ambrose Jr., W. G., Sen, A., Silyakova, A., & Carroll, J. (2018). Methane cold seeps as biological oases in the high-Arctic deep sea. *Limnology and Oceanography*, 63(Suppl. 1), S209–S231. <https://doi.org/10.1002/LNO.10732>
- Becker, E. L., Cordes, E. E., Macko, S. A., & Fisher, C. R. (2009). Importance of seep primary production to *Lophelia pertusa* and associated fauna in the Gulf of Mexico. *Deep-Sea Research Part I: Oceanographic Research Papers*, 56(5), 786–800. <https://doi.org/10.1016/j.dsr.2008.12.006>
- Bolyen, E., Rideout, J. R., Dillon, M. R., Bokulich, N. A., Abnet, C. C., al-Ghalith, G. A., Alexander, H., Alm, E. J., Arumugam, M., Asnicar, F., Bai, Y., Bisanz, J. E., Bittinger, K., Brejnrod, A., Brislawn, C. J., Brown, C. T., Callahan, B. J., Caraballo-Rodriguez, A. M., Chase, J., ... Caporaso, J. G. (2019). Reproducible, interactive, scalable and extensible microbiome data science using QIIME 2. *Nature Biotechnology*, 37, 852–857. <https://doi.org/10.1038/s41587-019-0209-9>
- Breiman, L. (2001). Random forests. *Machine Learning*, 45(1), 5–32. <https://doi.org/10.1023/A:1010933404324>
- Burge, C. A., Mouchka, M. E., Harvell, C. D., & Roberts, S. (2013). Immune response of the Caribbean sea fan, *Gorgonia ventalina*, exposed to an *Aplanochytrium* parasite as revealed by transcriptome sequencing. *Frontiers in Physiology*, 4, 180. <https://doi.org/10.3389/fphys.2013.00180>
- Cheng, J., Hui, M., & Sha, Z. (2019). Transcriptomic analysis reveals insights into deep-sea adaptations of the dominant species, *Shinkaiia crosnieri* (Crustacea: Decapoda: Anomura), inhabiting both hydrothermal vents and cold seeps. *BMC Genomics*, 20(1), 388. <https://doi.org/10.1186/s12864-019-5753-7>
- Childress, J. J., Fisher, C. R., Brooks, J. M., Kennicutt, M. C., 2nd, Bidigare, R., & Anderson, A. E. (1986). A methanotrophic marine molluscan (*Bivalvia*, *Mytilidae*) symbiosis: Mussels fueled by gas. *Science*, 233(4770), 1306–1308. <https://doi.org/10.1126/science.233.4770.1306>
- Childress, J. J., & Girguis, P. R. (2011). The metabolic demands of endosymbiotic chemoautotrophic metabolism on host physiological capacities. *Journal of Experimental Biology*, 214(2), 312–325. <https://doi.org/10.1242/jeb.049023>
- Cho, W., & Shank, T. M. (2010). Incongruent patterns of genetic connectivity among four ophiuroid species with differing coral host specificity on North Atlantic seamounts. *Marine Ecology*, 31(Suppl. 1), 121–143. <https://doi.org/10.1111/j.1439-0485.2010.00395.x>
- Clark, M. R., Althaus, F., Schlacher, T. A., Williams, A., Bowden, D. A., & Rowden, A. A. (2016). The impacts of deep-sea fisheries on benthic

- communities: A review. *ICES Journal of Marine Science*, 73(Suppl. 1), i51–i69. <https://doi.org/10.1093/ICESJMS/FSV123>
- Cordes, E. E., McGinley, M. P., Podowski, E. L., Becker, E. L., Lessard-Pilon, S., Viada, S. T., & Fisher, C. R. (2008). Coral communities of the deep Gulf of Mexico. *Deep-Sea Research Part I: Oceanographic Research Papers*, 55(6), 777–787. <https://doi.org/10.1016/j.dsr.2008.03.005>
- De Cáceres, M., & Legendre, P. (2009). Associations between species and groups of sites: Indices and statistical inference. *Ecology*, 90(12), 3566–3574. <https://doi.org/10.1890/08-1823.1>
- DeLeo, D. M., Glazier, A., Herrera, S., Barkman, A., & Cordes, E. E. (2021). Transcriptomic responses of deep-sea corals experimentally exposed to crude oil and dispersant. *Frontiers in Marine Science*, 8, 649909. <https://doi.org/10.3389/FMARS.2021.649909>
- DeLeo, D. M., Herrera, S., Lengyel, S. D., Quattrini, A. M., Kulathinal, R. J., & Cordes, E. E. (2018). Gene expression profiling reveals deep-sea coral response to the deepwater horizon oil spill. *Molecular Ecology*, 27(20), 4066–4077. <https://doi.org/10.1111/mec.14847>
- Demopoulos, A. W. J., Bourque, J. R., Cordes, E., & Stamler, K. M. (2016). Impacts of the deepwater horizon oil spill on deep-sea coral-associated sediment communities. *Marine Ecology Progress Series*, 561, 51–68. <https://doi.org/10.3354/meps11905>
- Deng, Y., Chen, F., Li, N., Jin, M., Cao, J., Chen, H., Zhou, Y., Wu, C., Zhuang, C., Zhao, Y., & Cheng, S. (2019). Cold-water corals in gas hydrate drilling cores from the South China Sea: Occurrences, geochemical characteristics and their relationship to methane seepages. *Minerals*, 9(12), 742. <https://doi.org/10.3390/min9120742>
- Doughty, C. L., Quattrini, A. M., & Cordes, E. E. (2014). Insights into the population dynamics of the deep-sea coral genus *Paramuricea* in the Gulf of Mexico. *Deep-Sea Research Part II: Topical Studies in Oceanography*, 99, 71–82. <https://doi.org/10.1016/j.dsr2.2013.05.023>
- Fisher, C., Roberts, H., Cordes, E., & Bernard, B. (2007). Cold seeps and associated communities of the gulf of Mexico. *Oceanography*, 20, 118–129. <https://doi.org/10.5670/oceanog.2007.12>
- Franco, N. R., Giraldo, M. Á., López-Alvarez, D., Gallo-Franco, J. J., Dueñas, L. F., Puentes, V., & Castillo, A. (2020). Bacterial composition and diversity in deep-sea sediments from the southern Colombian Caribbean Sea. *Diversity*, 13, 10. <https://doi.org/10.3390/D13010010>
- Galand, P. E., Remize, M., Meistertzheim, A. L., Pruski, A. M., Peru, E., Suhrhoff, T. J., le Bris, N., Vétiou, G., & Lartaud, F. (2020). Diet shapes cold-water corals bacterial communities. *Environmental Microbiology*, 22(1), 354–368. <https://doi.org/10.1111/1462-2920.14852>
- Girard, F., Cruz, R., Glickman, O., Harpster, T., & Fisher, C. R. (2019). In situ growth of deep-sea octocorals after the deepwater horizon oil spill. *Elementa: Science of the Anthropocene*, 7(1), 12. <https://doi.org/10.1525/elementa.349>
- Girard, F., & Fisher, C. R. (2018). Long-term impact of the deepwater horizon oil spill on deep-sea corals detected after seven years of monitoring. *Biological Conservation*, 225, 117–127. <https://doi.org/10.1016/j.biocon.2018.06.028>
- Girard, F., Fu, B., & Fisher, C. R. (2016). Mutualistic symbiosis with ophiuroids limited the impact of the deepwater horizon oil spill on deep-sea octocorals. *Marine Ecology Progress Series*, 549, 89–98. <https://doi.org/10.3354/meps11697>
- Girard, F., Shea, K., & Fisher, C. R. (2018). Projecting the recovery of a longlived deep-sea coral species after the deepwater horizon oil spill using state-structured models. *Journal of Applied Ecology*, 55, 1812–1822. <https://doi.org/10.1111/1365-2664.13141>
- Goffredi, S. K., Motooka, C., Fike, D. A., Gusmão, L. C., Tilic, E., Rouse, G. W., & Rodríguez, E. (2021). Mixotrophic chemosynthesis in a deep-sea anemone from hydrothermal vents in the Pescadero Basin, Gulf of California. *BMC Biology*, 19(1), 1–18. <https://doi.org/10.1186/s12915-020-00921-1>
- Guzman, H. M., Kaiser, S., & Weil, E. (2020). Assessing the long-term effects of a catastrophic oil spill on subtidal coral reef communities off the Caribbean coast of Panama (1985–2017). *Marine Biodiversity*, 50(3), 1–19. <https://doi.org/10.1007/S12526-020-01057-9/TABLES/4>
- Hadfield, J. D. (2010). MCMC methods for multi-response generalized linear mixed models: The MCMCglmm R package. *Journal of Statistical Software*, 33(2), 1–22. <https://doi.org/10.18637/jss.v033.i02>
- Hovland, M., & Thomsen, E. (1997). Cold-water corals—are they hydrocarbon seep related? *Marine Geology*, 137, 159–164. [https://doi.org/10.1016/S0025-3227\(96\)00086-2](https://doi.org/10.1016/S0025-3227(96)00086-2)
- Hu, Y.-J., & Satten, G. A. (2019). Testing hypotheses about the microbiome using the linear decomposition model. *bioRxiv*. <https://doi.org/10.1101/229831>
- Joye, S. B. (2020). The geology and biogeochemistry of hydrocarbon seeps. *Annual Review of Earth and Planetary Sciences*, 48, 205–231. <https://doi.org/10.1146/annurev-earth-063016-020052>
- Joye, S. B., Boetius, A., Orcutt, B. N., Montoya, J. P., Schulz, H. N., Erickson, M. J., & Lugo, S. K. (2004). The anaerobic oxidation of methane and sulfate reduction in sediments from Gulf of Mexico cold seeps. *Chemical Geology*, 205(3–4), 219–238. <https://doi.org/10.1016/j.chemgeo.2003.12.019>
- Kellogg, C. A., & Pratte, Z. A. (2021). Unexpected diversity of Endozoicomonas in deep-sea corals. *Marine Ecology Progress Series*, 673, 1–15. <https://doi.org/10.3354/MEPS13844>
- Kennicutt, M. C. (2017). Oil and gas seeps in the Gulf of Mexico. In *Habitats and biota of the Gulf of Mexico: Before the deepwater horizon oil spill*. https://doi.org/10.1007/978-1-4939-3447-8_5
- La Rivière, M., Garrabou, J., & Bally, M. (2015). Evidence for host specificity among dominant bacterial symbionts in temperate gorgonian corals. *Coral Reefs*, 34(4), 1087–1098. <https://doi.org/10.1007/s00338-015-1334-7>
- Laso-Pérez, R., Hahn, C., van Vliet, D., Tegetmeyer, H. E., Schubotz, F., Smit, N. T., Pape, T., Sahling, H., Bohrmann, G., Boetius, A., Knittel, K., & Wegener, G. (2019). Anaerobic degradation of non-methane alkanes by “candidatus methanoliparia” in hydrocarbon seeps of the gulf of Mexico. *mBio*, 10(4). <https://doi.org/10.1128/mBio.01814-19>
- Lewis, J. P., Tarnecki, J. H., Garner, S. B., Chagaris, D. D., & Patterson, W. F., III. (2020). Changes in reef fish community structure following the deepwater horizon oil spill. *Scientific Reports*, 10(1), 1–13. <https://doi.org/10.1038/s41598-020-62574-y>
- Love, M. I., Huber, W., & Anders, S. (2014). Moderated estimation of fold change and dispersion for RNA-seq data with DESeq2. *Genome Biology*, 15, 550. <https://doi.org/10.1186/s13059-014-0550-8>
- Luter, H. M., Whalan, S., Andreakis, N., Abdul Wahab, M., Botté, E. S., Negri, A. P., & Webster, N. S. (2019). The effects of crude oil and dispersant on the larval sponge holobiont. *ASM Journals*, 4(6). <https://doi.org/10.1128/mSystems.00743-19>
- McClain, C. R., Nunnally, C., & Benfield, M. C. (2019). Persistent and substantial impacts of the deepwater horizon oil spill on deep-sea megafauna. *Royal Society Open Science*, 6(8), 191164. <https://doi.org/10.1098/rsos.191164>
- McClain-Counts, J. P., Demopoulos, A. W. J., & Ross, S. W. (2017). Trophic structure of mesopelagic fishes in the Gulf of Mexico revealed by gut content and stable isotope analyses. *Marine Ecology*, 38(4), e12449. <https://doi.org/10.1111/MAEC.12449>
- Meistertzheim, A. L., Lartaud, F., Arnaud-Haond, S., Kalenitchenko, D., Bessalam, M., le Bris, N., & Galand, P. E. (2016). Patterns of bacteria-host associations suggest different ecological strategies between two reef building cold-water coral species. *Deep-Sea Research Part I: Oceanographic Research Papers*, 114, 12–22. <https://doi.org/10.1016/j.dsr.2016.04.013>
- Middelburg, J. J., Mueller, C. E., Veuger, B., Larsson, A. I., Form, A., & Oevelen, D. (2015). Discovery of symbiotic nitrogen fixation and chemoautotrophy in cold-water corals. *Scientific Reports*, 5(1), 1–9. <https://doi.org/10.1038/srep17962>
- Morris, R. M., & Spietz, R. L. (2022). The physiology and biogeochemistry of SUP05. *Annual Reviews*, 14, 261–275. <https://doi.org/10.1146/ANNUREV-MARINE-010419-010814>

- Mosher, C. V., & Watling, L. (2009). Partners for life: A brittle star and its octocoral host. *Marine Ecology Progress Series*, 397, 81–88. <https://doi.org/10.3354/MEPS08113>
- Neave, M. J., Apprill, A., Ferrier-Pagès, C., & Voolstra, C. R. (2016). Diversity and function of prevalent symbiotic marine bacteria in the genus *Endozoicomonas*. *Applied Microbiology and Biotechnology*, 100(19), 8315–8324. <https://doi.org/10.1007/s00253-016-7777-0>
- Niemann, H., Linke, P., Knittel, K., MacPherson, E., Boetius, A., Brückmann, W., Larvik, G., Wallmann, K., Schacht, U., Omeregje, E., Hilton, D., Brown, K., & Rehder, G. (2013). Methane-carbon flow into the benthic food web at cold seeps—A case study from the Costa Rica subduction zone. *PLoS One*, 8(10), e74894. <https://doi.org/10.1371/journal.pone.0074894>
- Oldach, M. J., Workentine, M., Matz, M. V., Fan, T. Y., & Vize, P. D. (2017). Transcriptome dynamics over a lunar month in a broadcast spawning acroporid coral. *Molecular Ecology*, 26(9), 2514–2526. <https://doi.org/10.1111/MEC.14043>
- Osman, E. O., Suggett, D. J., Voolstra, C. R., Pettay, D. T., Clark, D. R., Pogoreutz, C., Sampayo, E. M., Warner, M. E., & Smith, D. J. (2020). Coral microbiome composition along the northern Red Sea suggests high plasticity of bacterial and specificity of endosymbiotic dinoflagellate communities. *Microbiome*, 8(1), 8. <https://doi.org/10.1186/s40168-019-0776-5>
- Osman, E. O., & Weinnig, A. M. (2022). Microbiomes and obligate symbiosis of deep-sea animals. *Annual Review of Animal Biosciences*, 10(1), 151–176. <https://doi.org/10.1146/annurev-animal-081621-112021>
- Patro, R., Duggal, G., Love, M. I., Irizarry, R. A., & Kingsford, C. (2017). Salmon provides fast and bias-aware quantification of transcript expression. *Nature Methods*, 14, 417–419. <https://doi.org/10.1038/nmeth.4197>
- Polato, N. R., Vera, J. C., & Baums, I. B. (2011). Gene discovery in the threatened Elkhorn coral: 454 sequencing of the acropora palmata transcriptome. *PLoS One*, 6, e28634. <https://doi.org/10.1371/journal.pone.0028634>
- Quattrini, A. M., Herrera, S., Adams, J. M., Grinyó, J., Allcock, A. L., Shuler, A., Wirshing, H. H., Cordes, E. E., & McFadden, C. S. (2022). Phylogeography of *Paramuricea*: The role of depth and water mass in the evolution and distribution of deep-sea corals. *Frontiers in Marine Science*, 9, 849402. <https://doi.org/10.3389/fmars.2022.849402>
- Quattrini, A. M., Georgian, S. E., Byrnes, L., Stevens, A., Falco, R., & Cordes, E. E. (2013). Niche divergence by deep-sea octocorals in the genus *Callogorgia* across the continental slope of the Gulf of Mexico. *Molecular Ecology*, 22(15), 4123–4140. <https://doi.org/10.1111/mec.12370>
- R Development Core Team. (2017). *R: A language and environment for statistical computing*. R Foundation for Statistical Computing. <https://doi.org/10.1007/978-3-540-74686-7>
- Rincón-Tomás, B., Duda, J. P., Somoza, L., González, F. J., Schneider, D., Medialdea, T., Santofimia, E., López-Pamo, E., Madureira, P., Hoppert, M., & Reitner, J. (2019). Cold-water corals and hydrocarbon-rich seepage in Pompeia Province (Gulf of Cádiz)—Living on the edge. *Biogeosciences*, 16(7), 1607–1627. <https://doi.org/10.5194/bg-16-1607-2019>
- Rodriguez-Lanetty, M., Granados-Cifuentes, C., Barberan, A., Bellantuono, A. J., & Bastidas, C. (2013). Ecological inferences from a deep screening of the complex bacterial consortia associated with the coral, *Porites astreoides*. *Molecular Ecology*, 22, 4349–4362. <https://doi.org/10.1111/mec.12392>
- Rogers, K. L., Bosman, S. H., Wildermann, N., Rosenheim, B. E., Montoya, J. P., Hollander, D., Zhao, T., & Chanton, J. P. (2021). Mapping spatial and temporal variation of seafloor organic matter $\Delta^{14}\text{C}$ and $\delta^{13}\text{C}$ in the northern Gulf of Mexico following the deepwater horizon oil spill. *Marine Pollution Bulletin*, 164, 112076. <https://doi.org/10.1016/j.marpolbul.2021.112076>
- Ruiz-Jones, L. J., & Palumbi, S. R. (2017). Tidal heat pulses on a reef trigger a fine-tuned transcriptional response in corals to maintain homeostasis. *Science Advances*, 3(3). <https://doi.org/10.1126/sciadv.160129>
- Sogin, E. M., Leisch, N., & Dubilier, N. (2020). Chemosynthetic symbioses. *Current Biology*, 30(19), R1137–R1142. <https://doi.org/10.1016/j.cub.2020.07.050>
- Thresher, R. E., Guinotte, J. M., Matear, R. J., & Hobday, A. J. (2015). Options for managing impacts of climate change on a deep-sea community. *Nature Climate Change*, 5(7), 635–639. <https://doi.org/10.1038/nclimate2611>
- Turner, N. R., & Renegar, D. A. (2017). Petroleum hydrocarbon toxicity to corals: A review. *Marine Pollution Bulletin*, 119, 1–16. <https://doi.org/10.1016/j.marpolbul.2017.04.050>
- van de Water, J. A. J. M., Allemand, D., & Ferrier-Pagès, C. (2018). Host-microbe interactions in octocoral holobionts—Recent advances and perspectives. *Microbiome*, 6, 1–28. <https://doi.org/10.1186/s40168-018-0431-6>
- van de Water, J. A. J. M., Melkonian, R., Voolstra, C. R., Junca, H., Beraud, E., Allemand, D., & Ferrier-Pagès, C. (2017). Comparative assessment of Mediterranean gorgonian-associated microbial communities reveals conserved Core and locally variant bacteria. *Microbial Ecology*, 73(2), 466–478. <https://doi.org/10.1007/s00248-016-0858-x>
- Vohsen, S. A., Gruber-Vodicka, H. R., Osman, E. O., Saxton, M. A., Joye, S. B., Dubilier, N., Fisher, C. R., & Baums, I. B. (2020). Deep-sea corals near cold seeps associate with chemoautotrophic bacteria that are related to the symbionts of cold seep and hydrothermal vent mussels. *bioRxiv*. <https://doi.org/10.1101/2020.02.27.968453>
- Vohsen, S. A., Gruber-Vodicka, H. R., Meyer, M., Sadowski, M., Dubilier, N., Fisher, C. R., & Baums, I. B. (2022). The deep-sea coral, *Callogorgia delta*, associates with bacteria belonging to a novel marine branch of the Mollicutes. *bioRxiv*, 2022.10.07.511369. <https://doi.org/10.1101/2022.10.07.511369>
- Wang, Y., & LêCao, K.-A. (2019). Managing batch effects in microbiome data. *Briefings in Bioinformatics*, 21, 1954–1970. <https://doi.org/10.1093/bib/bbz105>
- Weinnig, A. M., Gómez, C. E., Hallaj, A., & Cordes, E. E. (2020). Cold-water coral (*Lophelia pertusa*) response to multiple stressors: High temperature affects recovery from short-term pollution exposure. *Scientific Reports*, 10(1), 1–13. <https://doi.org/10.1038/s41598-020-58556-9>
- Wong, Y. H., Sun, J., He, L. S., Chen, L. G., Qiu, J. W., & Qian, P. Y. (2015). High-throughput transcriptome sequencing of the cold seep mussel *Bathymodiolus platifrons*. *Scientific Reports*, 5(1), 1–15. <https://doi.org/10.1038/srep16597>
- Xu, A., Chen, Z., Qu, Y., Tian, Y., Shu, C., Zheng, X., Li, G., Yan, W., & Zhao, M. (2019). Cold-water corals in a cold seep area on the northern continental slopes of the South China Sea and their isotopic characteristics. *Deep-Sea Research Part I: Oceanographic Research Papers*, 152, 103043. <https://doi.org/10.1016/j.dsr.2019.05.003>

SUPPORTING INFORMATION

Additional supporting information can be found online in the Supporting Information section at the end of this article.

How to cite this article: Osman, E. O., Vohsen, S. A., Girard, F., Cruz, R., Glickman, O., Bullock, L. M., Anderson, K. E., Weinnig, A. M., Cordes, E. E., Fisher, C. R., & Baums, I. B. (2023). Capacity of deep-sea corals to obtain nutrition from cold seeps aligned with microbiome reorganization. *Global Change Biology*, 29, 189–205. <https://doi.org/10.1111/gcb.16447>